

POLITECNICO DI MILANO
Scuola di Ingegneria Industriale e dell'Informazione
Corso di Laurea Magistrale in Ingegneria Elettronica
Dipartimento di Elettronica, Informazione e Bioingegneria



MODEL AND CONTROL OF AN IN-WHEEL BRUSHLESS MOTOR

Relatore: Prof. Giambattista GRUOSO

Tesi di laurea di:
Stefano BIANCHI Matr. 851038

Anno Accademico 2016–2017

*For my family,
who always supports me
to reach my dreams... .*

-Stefano Bianchi -

Curiosity is all you need in life and if you are curious enough, you're gonna find your passions. And results who you get are just a logical consequence of how much passion you put on your life.

-Alex Zanardi-

Ringraziamenti

Questi sei anni universitari sono stati per me molto formativi, sia scolasticamente, che personalmente e umanamente. Nonostante una facoltà tecnica e scientifica basata sui numeri ho potuto capire che nella vita la differenza la fanno le persone che incontriamo.

Vorrei quindi ringraziare i professori Giambattista Gruosso e Luca Bascetta per la pazienza con cui mi hanno seguito e per tutte le indicazioni necessarie per completare questo lavoro.

Ringrazio anche Arturo Montúfar per gli insegnamenti nei mesi in cui abbiamo collaborato al progetto.

Vorrei ringraziare i miei genitori per essere sempre stati i miei sostenitori numero uno, per avermi dato la possibilità di arrivare fino a questo punto e perchè so che mi supporteranno sempre e comunque; sperando che possa ripagare almeno in piccola parte i vostri sacrifici rendendovi orgogliosi di me, e di ciò che grazie a voi ho potuto realizzare.

Un ringraziamento anche a tutta la mia famiglia: dai nonni, agli zii e ai cugini, ognuno di voi ha contribuito a suo modo al raggiungimento di questo mio traguardo.

Un grazie speciale alla mia sorellina, da quel 19 Giugno ne abbiamo passate tante, sono stati molti i litigi ma anche i bei momenti che ci hanno permesso di crescere insieme. Sono contento di averti avuto al mio fianco tutti questi anni, e so che non te lo dico abbastanza: ti voglio bene.

Tornando a casa ogni giorno dall'università è sempre bello trovare un amico che ti supporti e sopporti nei giorni peggiori o con cui festeggiare in quelli migliore, grazie a tutti i miei coinquilini, sia a quelli attuali (Casone, Bomby, Zio Dam, Nico e Cat) che a quelli degli anni passati (Mathias, Salino, Marco e Rik).

Un gruppo di amici speciali, che fin da piccoli ti sono sempre stati accanto, è difficile da trovare. Grazie per esserci sempre stati a Ricky, Spesly, Bonda, Pulkas, Montre e Manu.

Importante è stato anche l'imparare a lavorare in un team, ringrazio tutti coloro con cui ho condiviso attività e progetti: il gruppo degli animatori, le ragazze e i ragazzi di CurtaTune, gli amici del karate e tutti i membri del Team DynamiΣ.

Abstract

The purpose of this thesis is to realize a MATLAB/Simulink model of an in-wheel motor: the system includes a motor inside the wheel, electronics necessary to energize the motor and the control strategy to make it move at desired speed or with a specific torque. There was applied two different control strategy on the wheel: one considering the motor with sinusoidal back electromotive Force and the other considering the motor with Trapezoidal BEMF. The real motor, after a simple test, has proven to have sinusoidal BEMF. However both strategy can be still used.

Chapter 1 is about Brushless motor, it is explained its principle of operation and 2 kinds of motors are distinguished; furthermore control strategy most used are introduced. In Chapter 2 it is analyzed the problem of calculation and estimation of motor's parameters. After determination of parameters needed for simulation, they are validated through some simulation. Chapter 3 is about field oriented control, it is shown the model and it is compared to experimental data. Established that the model is an enough good approximation of the real system, parameters of controllers are calculated and compared. Chapter 4 is structured as Chapter 3 but relatively to the Trapezoidal Control. Finally in Chapter 5 there is a short comparison between control strategy seen in chapters before to define which is better.

Results showed that Simulink model has a behavior very similar to the real motor despite simplifications mandatory in modeling process. This kind of result is valid with both control strategy. Comparisons between control strategy show that Foc should be preferable to 6-Step commutation, as expected by BEMF shapes. More consideration can be done with the real motor: sensors in simulation (to read currents and position) are considered ideal, in real word sensors introduce delays and noise not yet considered in this simulation.

Sommario

L'obiettivo di questa tesi è quello di realizzare un modello in MATLAB/Simulink di una motoruota: un sistema che comprendente un motore brushless «in-wheel», l'elettronica necessaria al funzionamento del motore e il sistema di controllo che ci permette di far ruotare la motoruota ad una determinata velocità o di applicare una determinata coppia. Sono state attuate due diverse strategie di controllo considerando le due principali forme di forza controelettromotrice nei motori brushless: sinusoidale e trapezoidale. Il profilo della forza controelettromotrice del motore è stato verificato essere sinusoidale, ma entrambe le strategie di controllo rimangono attuabili.

Il Capitolo 1 è dedicato al motore brushless: viene spiegato il principio di funzionamento e vengono distinti i due tipi di motore brushless comunemente usati; vengono inoltre presentate le due tecniche utilizzate per controllarli. Nel Capitolo 2 viene trattato il problema della determinazione e della stima dei parametri del motore. Dopo aver determinato i parametri necessari per la simulazione questi vengono validati anche tramite simulazione. Il Capitolo 3 è dedicato al sistema di controllo vettoriale, viene presentato il modello utilizzato e viene confrontato con i dati sperimentali. Una volta appurato che il modello approssima correttamente il funzionamento del motore reale vengono calcolati i parametri dei controllori e simulati. Il Capitolo 4 è analogo al terzo ma la strategia di controllo utilizzata sarà invece quella trapezoidale. Infine nel capitolo 5 vengono confrontate le simulazioni utilizzando le 2 tecniche trattate nei capitoli precedenti per poter definire quale tecnica è più conveniente.

I risultati ottenuti mostrano che il modello Simulink ha un comportamento molto simile a quello del motore reale nonostante le semplificazioni risultate obbligatorie nella fase di modellazione. Questo è risultato valido con entrambe le tecniche di controllo. Il confronto tra queste in fase di simulazione mostra che è preferibile un controllo vettoriale, come ci si può aspettare conoscendo le forme delle forze controelettromotrici. Ulteriori considerazioni possono essere fatte utilizzando il motore reale: i sensori utilizzati nella simulazione (per correnti e posizione) sono ideali, i sensori reali introducono invece ritardi e rumore non considerati.

Contents

Introduction	1
1 Brushless Motor	5
1.1 Operating principle	5
1.2 Trapezoidal Brushless Motor	6
1.2.1 6-Step BLDC motor control	6
1.2.2 Hall Effect Sensor	6
1.2.3 Torque generated by the Motor	7
1.3 Sinusoidal Brushless Motor	10
1.3.1 Torque generated by the Motor	10
1.3.2 6-step Commutation applied on a sinusoidal motor	12
1.3.3 Current Control in a Brushless Motor	12
2 Estimation and Validation of parameters	17
2.1 Resistance and Inductance of the Motor	17
2.2 Flux Linkage	20
2.3 Friction of the Motor	21
2.4 Inertia of the Motor	21
2.5 Parameters with Load	25
2.5.1 Friction with Load	25
2.5.2 Inertia with Load	26
3 Field Oriented Control Model	27
3.1 Simulink Model	27
3.1.1 Mechanical	27
3.1.2 Electrical	28
3.1.3 Control	29
3.2 Simplified Model	30
3.3 Validation of the Model	32
3.4 Controller Parameters	39
3.4.1 Current Loop	39
3.4.2 Speed Loop	41

4 Brushless DC Control Model	45
4.1 Simulink Model	45
4.1.1 Control	45
4.2 Simplified Model	47
4.3 Validation of the Model	49
4.4 Controller Parameters	63
4.4.1 Current Loop	63
4.4.2 Speed Loop	65
5 Comparison between FOC and 6-Step	67
5.1 Speed Step Response Comparison	67
5.2 Comparison at Regime	69
5.3 Choise of Control Strategy	69
Conclusions	71
Bibliography	72
Bibliography	73

List of Figures

1	The first Davenport motor	1
2	Division of electric motors	2
1.1	Brushless Motor	5
1.2	Comparison BEMF in Sinusoidal and Trapezoidal Brushless Motor	6
1.3	Currents flowing through coils with 6-step commutation sequence	7
1.4	Windings in BLDC motor	8
1.5	Current and BEMF with 6-step commutation sequence	9
1.6	6-step commutation applied on a sinusoidal motor	13
1.7	Clarke Transformation	14
1.8	Park Transforamtion	15
1.9	FOC Control Scheme	16
2.1	Current Loop scheme to estimate R_{phase} and L_{phase}	17
2.2	Quadrature Current Step Response to calculate R_{phase}	18
2.3	Phase Currents with $R_{phase}=186m\Omega$ and $L_{phase}=386\mu H$	19
2.4	Phase Currents with $R_{phase}=80m\Omega$ and $L_{phase}=380\mu H$	19
2.5	Phase Currents with $R_{phase}=113.8m\Omega$ and $L_{phase}=79.7\mu H$	20
2.6	Quadrature Currents Comparison to Validate R_{phase} and L_{phase}	20
2.7	Polynomial curve that approximate the Friction of the Motor	21
2.8	Constant Acceleration of 3 A to compare Inertia	24
2.9	Constant Acceleration with different Current Reference	24
2.10	Motor stopped by Friction to compare Inertia	25
2.11	Polynomial curve that approximate the Friction of the Motor with Load	26
2.12	Constant Acceleration to Validate Inertia with Load	26
3.1	Model of the System	27
3.2	Friction Model	28
3.3	Model of Inverter	29
3.4	Model of Controller	29
3.5	FOC and Speed Controller	30
3.6	Model of the System Simplified	30

3.7	Model of Controller Simplified	31
3.8	Comparison between complete and simplified models	31
3.9	Phase currents step response to quadrature current reference	32
3.10	Quadrature current step response to current reference	33
3.11	Speed step response to current reference 1A	33
3.12	Speed step response to current reference 2A	34
3.13	Speed step response to current reference 3A	34
3.14	Speed step response to current reference 3A with Load	35
3.15	Regime phase current with $i_q=2.5A$	35
3.16	Regime phase currents with $i_q=2.5A$	36
3.17	Regime phase current with $i_q=2.8A$	36
3.18	Regime phase currents with $i_q=2.8A$	37
3.19	Step Response 100 rpm	38
3.20	Step Response 200 rpm	38
3.21	Step Response 300 rpm	39
3.22	Current control loop	40
3.23	Step Response of quadrature current with different P and I values . .	41
3.24	Speed and Current Loop Nested	41
3.25	Speed and Current Loop Nested	42
3.26	Speed Step Response	43
3.27	Speed Step Response	43
4.1	Model of the System	45
4.2	Model of Controller	46
4.3	Speed Control BLDC	46
4.4	Speed Control BLDC with Current Loop	47
4.5	Model of the System Simplified	47
4.6	Model of Controller Simplified	48
4.7	Current Phase with Duty Cycle 10%	50
4.8	Comparison Current Phases with Duty Cycle 10%	50
4.9	Voltage Phase with Duty Cycle 10%	51
4.10	Comparison of Voltage Phases with Duty Cycle 10%	51
4.11	Tests with Duty Cycle 50%	52
4.12	Tests with Duty Cycle 90%	52
4.13	Current Phase with Duty Cycle 10% - With Load	53
4.14	Comparison Current Phases with Duty Cycle 10% -With Load . . .	53
4.15	Voltage Phase with Duty Cycle 10% - With Load	54
4.16	Comparison of Voltage Phases with Duty Cycle 10% - With Load . .	54
4.17	Tests with Duty Cycle 50% - With Load	55
4.18	Current Phase with Speed 100rpm	56

4.19 Comparison Current Phases with Speed 100 rpm	56
4.20 Voltage Phase with Speed 100rpm	57
4.21 Comparison of Voltage Phases with Speed 100 rpm	57
4.22 Tests with Speed 200 rpm	58
4.23 Tests with Speed 400 rpm	58
4.24 Current Phase with Speed 100rpm - With Load	59
4.25 Comparison Current Phases with Speed 100 rpm - With Load	59
4.26 Voltage Phase with Speed 100rpm - With Load	60
4.27 Comparison of Voltage Phases with Speed 100 rpm - With Load	60
4.28 Tests with Speed 200 rpm - With Load	61
4.29 Speed Step Response 100 rpm	62
4.30 Speed Step Response 200 rpm	62
4.31 Step Response of current with different P and I values	64
4.32 Speed Step Response with different PI Parameters	66
4.33 Speed Step Response with different PI Parameters - Detail	66
5.1 Speed Step Response with FOC and 6-Step	67
5.2 Torque during Step Response with FOC and 6-Step	68
5.3 Current phase during Speed Step Response with FOC and 6-Step	68
5.4 Torque at regime with FOC and 6-Step	69
5.5 Current Phase at regime with FOC and 6-Step	70

Introduction

Electric motors provide the driving power for a large and still increasing part of our modern industrial economy. The range of sizes and types of motors is large and the number and diversity application continues to expand. [2]

The electric motor was first developed in the 1830s, around 30 years after the first battery.

In 1834 Thomas Davenport of Vermont developed the first real electric motor, with 'real' meaning the first one powerful enough to do tasks. Others «motors» were created before by Joseph Henry and Michael Faraday, they were motion devices that work with magnetic field. The early motors created spinning disks or levers that rocked back and forth. These devices were «useless» because they weren't able to do any work for humankind, but they were important for leading the way to better motors in the future. Davenport's motors were able to run a model trolley on a circular track and other task. The trolley later turned out to be the first important application of electric power.



Figure 1: The first Davenport motor

After weak electrics motors developed by Henry and Faraday, another pioneer named Hippolyte Pixii figured out that running the motor backwards he could create

pulses of electricity. By 1860s powerful generators were being developed. Without generators electrical industry could not begin because batteries were not an economical way to power society's needs.

In the 1880s there was the important invention of the three-phase electric power system which is the basis for modern electrical power transmission and advanced electric motors. The three-phase synchronous motor, today, is used mostly in highly dynamic application and in electric cars. [4]

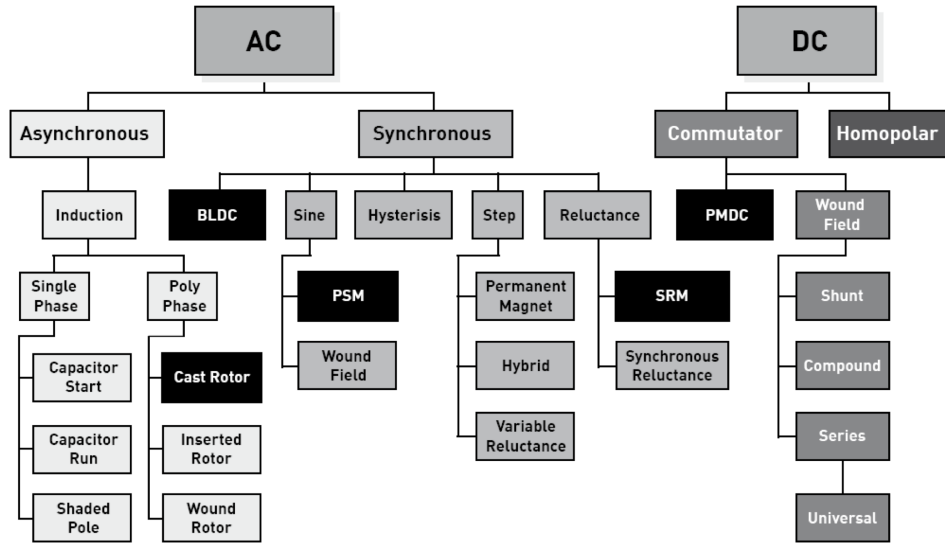


Figure 2: Division of electric motors

Nowadays electrical motor can be powered by direct current(DC) sources, such as from batteries, motor vehicles or rectifier, or by alternating current(AC) sources, such as from the power grid, inverters or generators. AC motor can be further divided in Synchronous and Asynchronous motors: synchronous motor is a machine whose rotor speed and the speed of stator magnetic field is equal, while asynchronous motor is a machine whose rotor rotates at the speed less than the synchronous speed. Last division we are interested in, is between brushed and brushless motor. In brushed motor there are brushes used to deliver current to the motor windings through commutator contacts. In brushless motors there is none of these currents carrying commutator, the field inside a brushless motor is switched via an amplifier triggered by a commutation device.

The purpose of this thesis is to realize a MATLAB/Simulink model of the system that include a motor inside the wheel, and the control strategy to make it move at desired speed or with a specific torque. There was applied 2 different control strategy on the wheel: one considering the motor with sinusoidal back electromotive Force and the other considering the motor with Trapezoidal BEMF. The real motor, after a simple test, has proven to have sinusoidal BEMF. However both strategy can be

still used.

In Chapter 1 it is explained the theory about Brushless motor and the way they are controlled, including difference between Trapezoidal and Sinusoidal motor. In Chapter 2 it is showed how parameters of the motor were calculated and estimated. In Chapter 3 is shown Field Oriented Control model and its validation with some tests. Chapter 4 is structured as Chapter 3 but relatively to the Trapezoidal Control. Finally in Chapter 5 there is a short comparison between these 2 strategy of control.

Introduction

Chapter 1

Brushless Motor

1.1 Operating principle

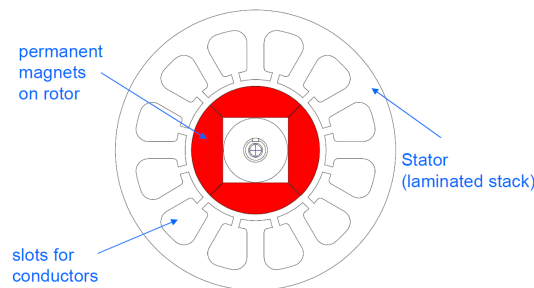


Figure 1.1: Brushless Motor

A Brushless motor is a Permanent magnet alternating current (PMAC) motor, it is a synchronous motor so the rotor and the magnetic field have the same angular speed. As we can see in Figure 1.1 permanent magnets are placed on the rotor, while windings of the phases (generally 3) are positioned on the stator. Phases are alternately powered to generate the magnetic field always orthogonal to the field of permanent magnets: the motor can be considered synchronous because of this orthogonality. To keep the motor synchronized is necessary commutate through an inverter currents in windings on the stator, based on the angular position of the rotor that can be read from a sensor. Brushless Motor are generally categorized into two types:

- Trapezoidal Brushless Motor (BLDC)
- Sinusoidal Brushless Motor (PMSM)

The principal difference we can see in these 2 categories is the Back Electromotive Force, and as we can see in Figure 1.2 is this characteristic that give the names at the 2 kinds of motors.

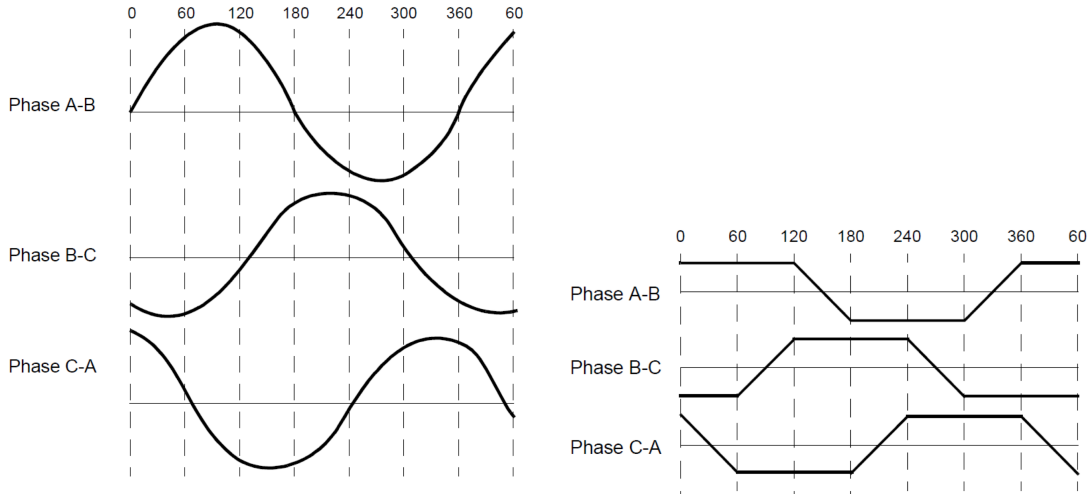


Figure 1.2: Comparison BEMF in Sinusoidal and Trapezoidal Brushless Motor

[1]

1.2 Trapezoidal Brushless Motor

1.2.1 6-Step BLDC motor control

The 6-step method is one of the simplest methods for driving 3-phase BLDC motors, the motor is driven by a three-phase inverter with six-step commutation depending on angular position of the rotor. Angular position can be detected with hall effect sensor but can also be derived from BEMF detection, in this case it is considered in sensorless mode. The logic of this commutation is to detect the rotor position then to energize the phases that will produce the most amount of torque.

The motor is driven energizing 2 phases at a time: the current enters in the first winding and exits in the second winding; third phase is left floating.

In Figure 1.3 it is possible to see how in the currents flow in the motor in each of 6 step commutation.

1.2.2 Hall Effect Sensor

The angular position in BLDC is generally read just through Hall effect sensors embedded into the stator. Whenever the rotor magnetic poles pass near the Hall sensor, they give a signal high or low depending on what pole is passed near the sensors. With 3 sensors we can detect angles with a step of 60° . This step is exactly what is needed to control a motor with a 6-step method.

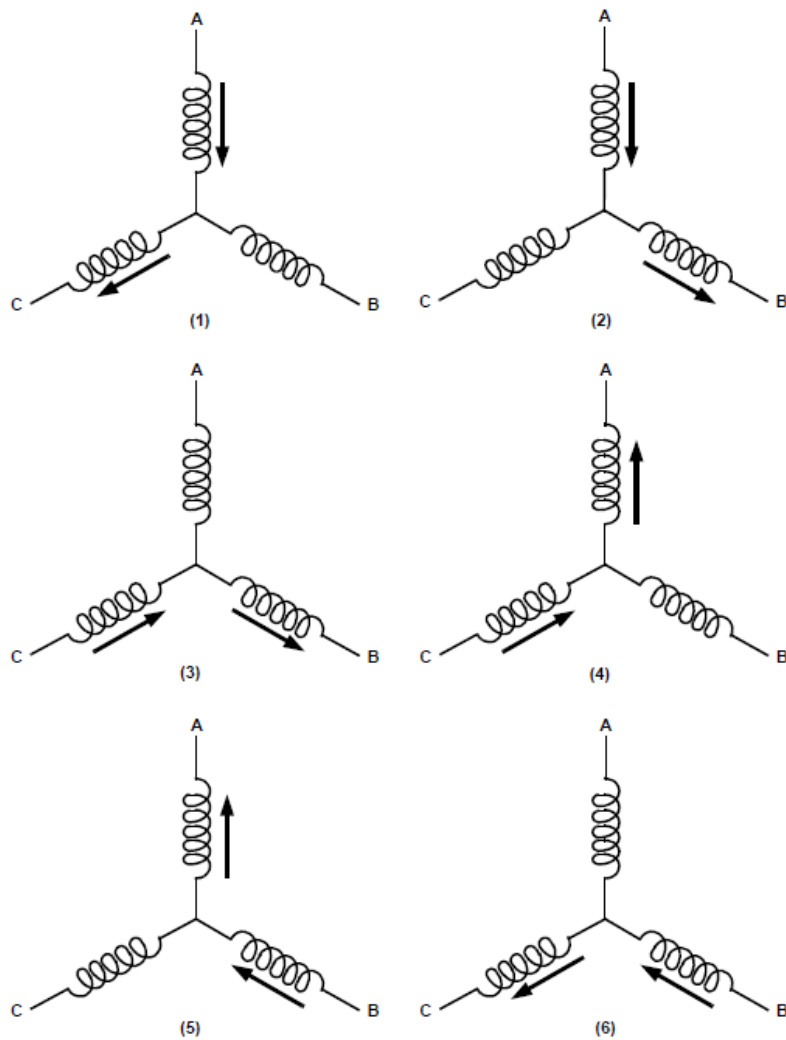


Figure 1.3: Currents flowing through coils with 6-step commutation sequence

1.2.3 Torque generated by the Motor

It is easy to calculate the torque generated: the electrical power absorbed by the motor and effectively converted in mechanical power is the product between currents in windings on stator and the BEMF applied on them. In particular with 3 different phases (a, b, c):

$$P_m = E_a I_a + E_b I_b + E_c I_c \quad (1.1)$$

Mechanical power equation is:

$$P_m = \tau_m \omega$$

so it can be obtained

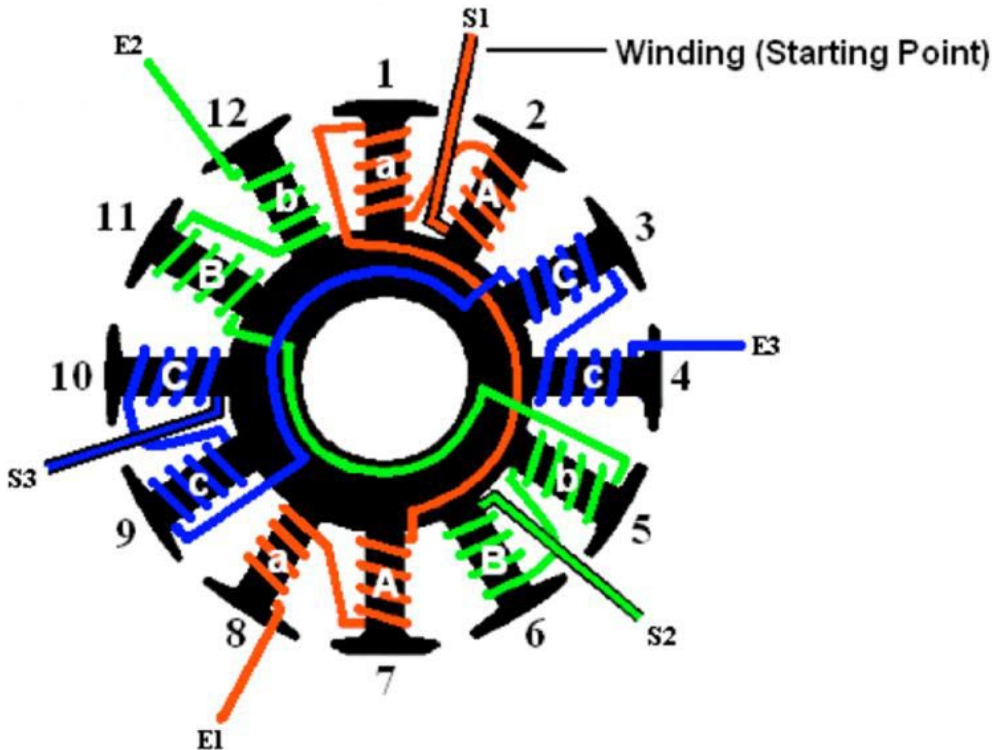


Figure 1.4: Windings in BLDC motor

$$\tau_m = \frac{E_a I_a + E_b I_b + E_c I_c}{\omega} \quad (1.2)$$

In figure 1.4 we can see for each phase, in each pole there are 2 windings. Considering the first phase A, on windings 1 and 2 there will be calculate 2 different BEMFs and then summed together to arrive at a unique BEMF for the phase A, which will have a trapezoidal shape.

BEMFs E_a , E_b and E_c can be easily obtained calculating the derivative respect the time of the flux linkage with every phase. Supposing a square wave of the flux density in the air gap, in function of angular position of the rotor, flux linkage with coil A change linearly with the position of rotor. Maximum Φ_{max} of flux linkage is related to angular position $\theta = 0^\circ$ (positive maximum) and $\theta = 180^\circ$ (negative maximum). Integrating magnetic field $B(\theta)$ in the air gap it is obtained:

$$\phi_{max} = Nrl \int_{-\pi/2}^{\pi/2} B(\theta) d\theta = Nrl \bar{B} \pi$$

where r is internal radius of stator, l the axial length of both rotor and stator and \bar{B} the value of magnetic field in the air gap. We can find the back electromotive force in the coil A as:

$$E_A = -\frac{d\phi_{m1}}{dt} = -\frac{d\phi_{mi}}{d\theta} \frac{d\theta}{dt} = -\omega \frac{d\phi_{m1}}{d\theta}$$

Expressing the derivative of the flux linkage respect the angle in function of maximum flux linkage it is obtained a square wave BEMF, which amplitude is:

$$\bar{E}_A = \frac{2\phi_{max}}{\pi} |\omega|$$

BEMF in coil a has the same expression but it is out of phase of 30° . When both coils are connected in series, the resulting BEMF will become trapezoidal. With real windings it is obtained for each phase a trapezoidal BEMF $E_i(\theta)$, with amplitude

$$\bar{E}_i = \frac{4\phi_{max}}{pi} |\omega|$$

With 6-step method current I_i are generated to follow back electromotive forces E_i like in Figure 1.5

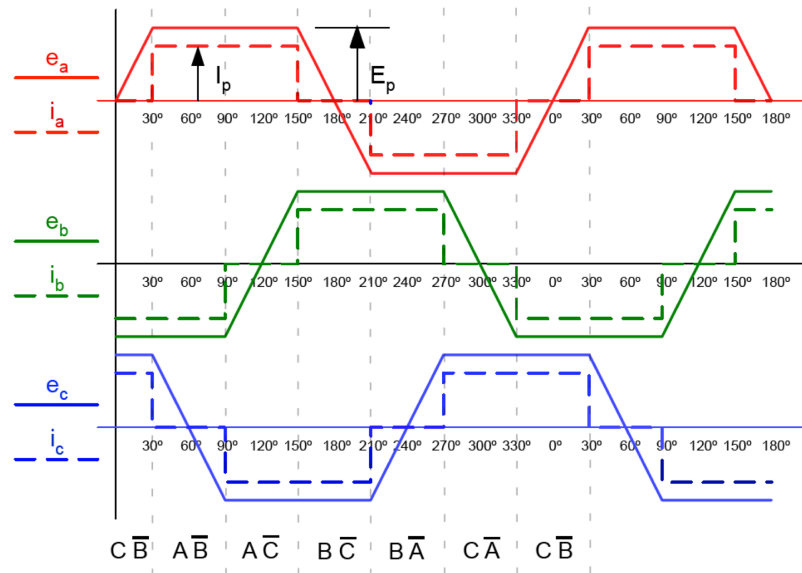


Figure 1.5: Current and BEMF with 6-step commutation sequence

At every moment 2 phases are always conducting the same current (with opposite sign because in the first phase the current is entering and in the second one is exiting), while the corresponding BEMF have the same value, but with opposite sign. Considering the 1.2 it can be obtained:

$$\tau_m = \frac{2E_i I_i}{\omega} = \frac{8\phi_{max}}{\pi} I = K_t I$$

Considering the three phases are generally Y-connected

$$I_a + I_b + I_c = 0 \quad (1.3)$$

the brushless motor model, relatively of electrical parameters, is defined by the equation 1.3 and by the following:

$$\begin{bmatrix} V_a \\ V_b \\ V_c \end{bmatrix} = \begin{bmatrix} R & 0 & 0 \\ 0 & R & 0 \\ 0 & 0 & R \end{bmatrix} \begin{bmatrix} I_a \\ I_b \\ I_c \end{bmatrix} + \frac{d}{dt} \left(\begin{bmatrix} L_a & M_{ab} & M_{ac} \\ M_{ba} & L_b & M_{bc} \\ M_{ca} & M_{cb} & L_c \end{bmatrix} \begin{bmatrix} I_a \\ I_b \\ I_c \end{bmatrix} \right) + \begin{bmatrix} E_a \\ E_b \\ E_c \end{bmatrix} + \begin{bmatrix} V_n \\ V_n \\ V_n \end{bmatrix} \quad (1.4)$$

where V_i are voltages applied to phases having as reference the ground of the inverter, V_n is the potential of neutral, R is the phase resistance, E_i are the back electromotive force and L_i , M_{ij} are respectively auto and mutual inductances of phase. Assuming reluctances of motors don't change with the angle, so L_i are equal and the same for M_{ij} , the considered equation 1.4 becomes:

$$\begin{bmatrix} V_a \\ V_b \\ V_c \end{bmatrix} = R \begin{bmatrix} I_a \\ I_b \\ I_c \end{bmatrix} + L \frac{d}{dt} \begin{bmatrix} I_a \\ I_b \\ I_c \end{bmatrix} + \begin{bmatrix} E_a \\ E_b \\ E_c \end{bmatrix} + \begin{bmatrix} V_n \\ V_n \\ V_n \end{bmatrix} \quad (1.5)$$

where $L = L_i - M_{ij}$.

1.3 Sinusoidal Brushless Motor

1.3.1 Torque generated by the Motor

Principal difference between a brushless trapezoidal motor and a sinusoidal one consist in the different shape function obtained in the back electromotive forces. In both cases the BEMFs can be expressed as a product of the angular speed by a shape function $K_i(\theta)$, so:

$$E_i = \omega K_i(\theta)$$

Configuring appropriately permanent magnets on the rotor is possible to obtain a sinusoidal distribution of the magnetic field, having the direction of maximum amplitude which rotate at the speed of the rotor. Considering the direction of maximum amplitude of the magnetic field as a reference mobile axis to measure the angles:

$$B(\varphi, \theta) = \bar{B} \cos(\varphi - \theta)$$

where φ represent a generic point in the air gap and θ is the rotation of the rotor.

Considering a sinusoidal distribution for conductors of each phase, in which in an infinitesimal angle $d\varphi$ are contained a number of conductor

$$dn = \frac{N_s}{2} \sin(\varphi) d\varphi$$

where N_s is the number of turns in the coil. We can calculate the flux linkage ϕ_m with the coil composed by dn conductor, furthermore we consider conductors return with an angle $-\varphi$

$$\phi_m = \int_{-\varphi}^{\varphi} B(\sigma, \theta) r l d\sigma = 2 \bar{B} r l \sin \varphi \cos \theta$$

Back electromotive force dE inducted by the coil composed by dn conductors will be

$$dE = -\frac{d\phi_m}{dt} dn = \bar{B} r l \omega N_s \sin^2 \varphi \sin \theta d\varphi$$

Overall back electromotive force E will be

$$E = \int_0^\pi dE = \omega \frac{\bar{B} r l N_s \pi}{2} \sin \theta = \omega K \sin \theta$$

Three phase have $\frac{2}{3}\pi$ of phase displacement, and considering the generic case having p polar pairs:

$$K_a(\alpha) = pK \sin(p\theta) = pK \sin(\alpha)$$

$$K_b(\alpha) = pK \sin(p\theta - 2\pi/3) = pK \sin(\alpha - 2\pi/3)$$

$$K_c(\alpha) = pK \sin(p\theta - 4\pi/3) = pK \sin(\alpha - 4\pi/3)$$

To obtain a constant torque independent from the angle we have to impose currents

$$I_a = I_a(\alpha) = I \sin(\alpha)$$

$$I_b = I_b(\alpha) = I \sin(\alpha - 2\pi/3)$$

$$I_c = I_c(\alpha) = I \sin(\alpha - 4\pi/3)$$

Considering the equation 1.2 :

$$\tau_m = pK I \sin^2 \alpha + pK I \sin^2(\alpha - 2\pi/3) + pK I \sin^2(\alpha - 4\pi/3) = \frac{2}{3} pK I = K_t I$$

Dynamic of electrical quantities is still described by equations 1.3 and 1.5 .

1.3.2 6-step Commutation applied on a sinusoidal motor

As it was said before 6-step commutation is an easy way to control a BLDC motor, but it is possible to apply this method to a sinusoidal motor. As we can see later the torque will present a ripple due to we are considering trapezoidal a BEMF that actually is Sinusoidal. [8]

In Figure 1.6 we can see the current applied on phases is the same applied on Figure 1.5, but the BEMF is sinusoidal, in both cases we apply a constant current in the 120° where BEMF is maximum.

Let's try to calculate the torque from each phase in a period of 60° . We can consider phases A and B conducting, and phase C floating, with positive value in phase A:

$$\begin{cases} \tau_a = pKI\sin(\theta) \\ \tau_b = pK(-I)\sin(\theta - \frac{2}{3}\pi) \\ \tau_c = 0 \end{cases}$$

$$\tau = pKI \left[\sin(\theta) - \sin(\theta - \frac{2}{3}\pi) \right] = -\sqrt{3}\sin(\theta + \frac{\pi}{6})KI \quad (1.6)$$

We can obtain

$$\tau_{max} = \sqrt{3}pKI$$

$$\tau_{avg} = 0.995\tau_{max}$$

and

$$\tau_{min} = 0.866\tau_{max}$$

1.3.3 Current Control in a Brushless Motor

In three phase brushless motor we have three different currents, one in each phase, we want to control, but considering the equation 1.3 we know the 3 phase currents aren't independent to each other. So it's enough control 2 of them and the third one will be uniquely determined by the Y -connection of the motor's phases.

In case of digital control is preferred, after an appropriate transformation of variables, change the model of the motor in order to eliminate the dependence from the electrical angle α . This technic is called Field Oriented Control.

From the point of view of control, brushed motors are the better machine: the main advantage is guaranteed by a situation of complete magnetic decoupling. It can be defined a polar axis, defined by permanent magnets, and a quadrature axis defined by magnetic field generated by armature currents. Furthermore these 2 axes are always orthogonal, independently to relative positon of the rotor respect the stator,

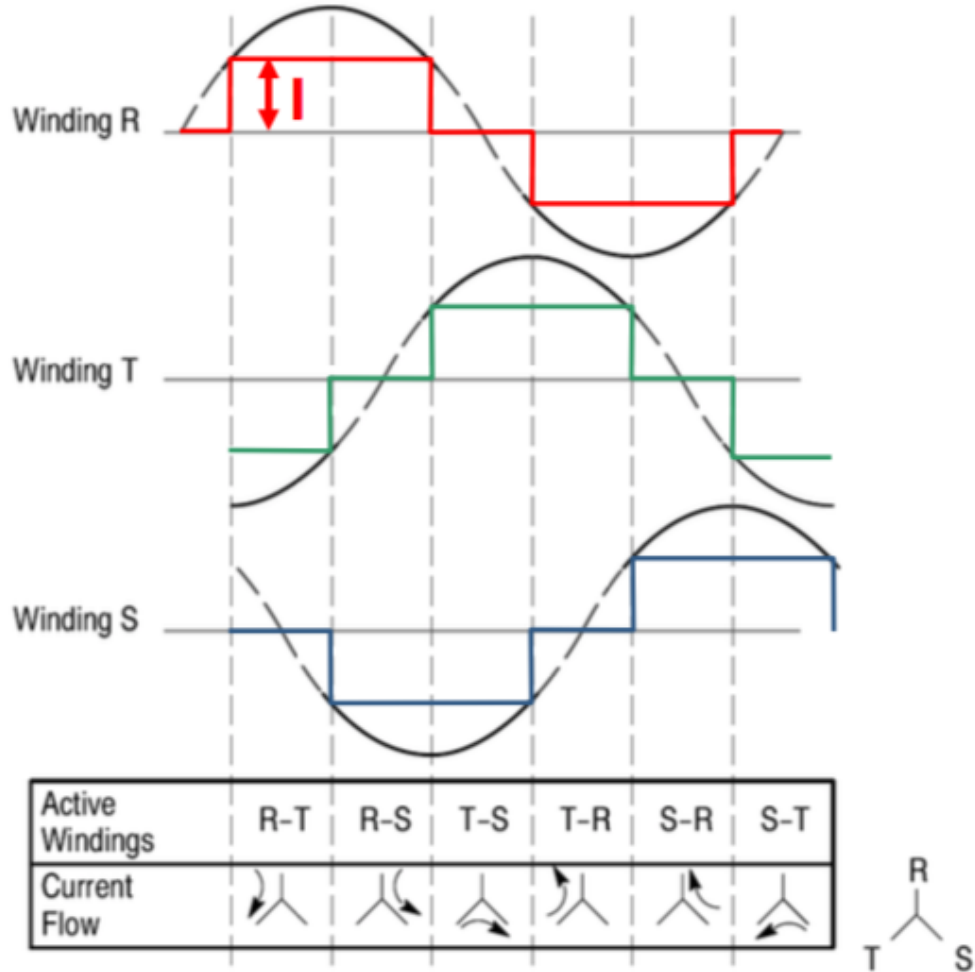


Figure 1.6: 6-step commutation applied on a sinusoidal motor

and independently from voltages applied on brushes. In case of brushless motor the squareness between axis of magnetic field generated by permanent magnets, and axis of magnetic field generated by currents in the stator is realized only with an appropriate modulation of phase currents. Because of this is not possible identify, with the model used until now, variables which act only on torque production. In case of brushless sinusoidal motor is needed a transformation that introduce new variables, defined in a reference jointly liable with the rotor, whose axes are respectively defined direct and quadrature axes.

In brushless motor direct axis is the axis of the magnetic field generated by permanents magnets. It is possible also associate to quadrature axis a fictitious power supply circuit, in which it would flow a current proportional to the torque we want to generate.

The transformation of variable can be done by 2 different transformation: Clarke

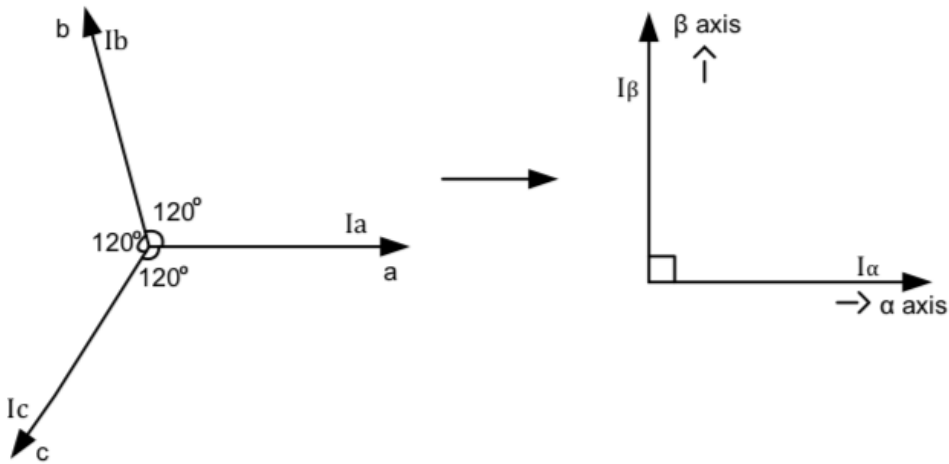


Figure 1.7: Clarke Transformation

and Park transformation.

Clarke Transformation

The purpose of this transformation is to translate three phase quantities from a three phase reference frame to the two axis orthogonal stationary reference frame as shown in Figure 1.7 . Clarke transformation is expressed by the following equations:

$$I_\alpha = \frac{2}{3}I_a - \frac{1}{3}(I_b - I_c)$$

$$I_\beta = \frac{2}{\sqrt{3}}(I_b - I_c)$$

Generally it easier consider $I_\alpha = I_a$, and considering the Y Connection with the equation 1.3 , the transformation can be considered

$$I_\alpha = I_a$$

$$I_\beta = \frac{1}{\sqrt{3}}(I_a + 2I_b)$$

The inverse Clarke transformation, needed when we want to apply desired voltages, is represent by equations:

$$V_a = V_\alpha$$

$$V_b = \frac{-V_\alpha + \sqrt{3}V_\beta}{2}$$

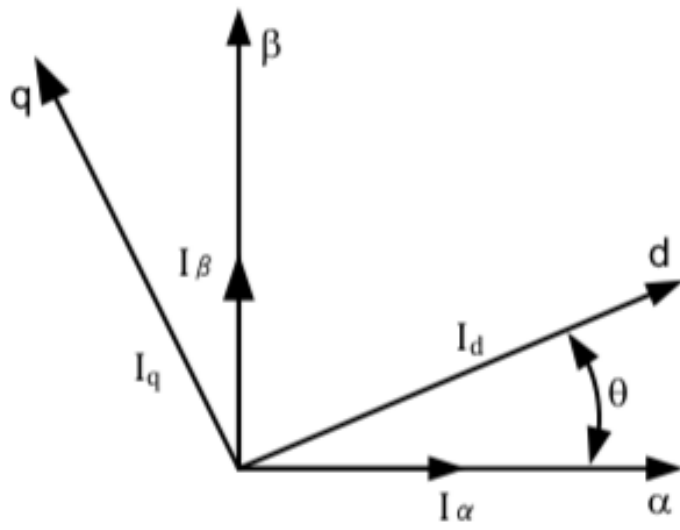


Figure 1.8: Park Transformation

$$V_c = \frac{-V_\alpha - \sqrt{3}V_\beta}{2}$$

Park Transformation

The purpose of Park transformation is to transform stationary reference frame quantities into rotating reference frame quantities as shown in Figure 1.8 . Park transformation is expressed by the following equations:

$$I_d = I_\alpha \cos(\theta) + I_\beta \sin(\theta)$$

$$I_q = I_\beta \cos(\theta) - I_\alpha \sin(\theta)$$

Inverse Park Transformation is represent by equations:

$$V_\alpha = V_d \cos(\theta) - V_q \sin(\theta)$$

$$V_\beta = V_q \cos(\theta) + V_d \sin(\theta)$$

Applying these 2 transformation to the equation 1.5 we can obtain:

$$V_d = RI_d + L \frac{dI_d}{dt} + p\omega LI_q$$

$$V_q = RI_q + L \frac{dI_q}{dt} - p\omega LI_d + pK\omega$$

In the new model there is no more a dependency on electric angle, but it appeared

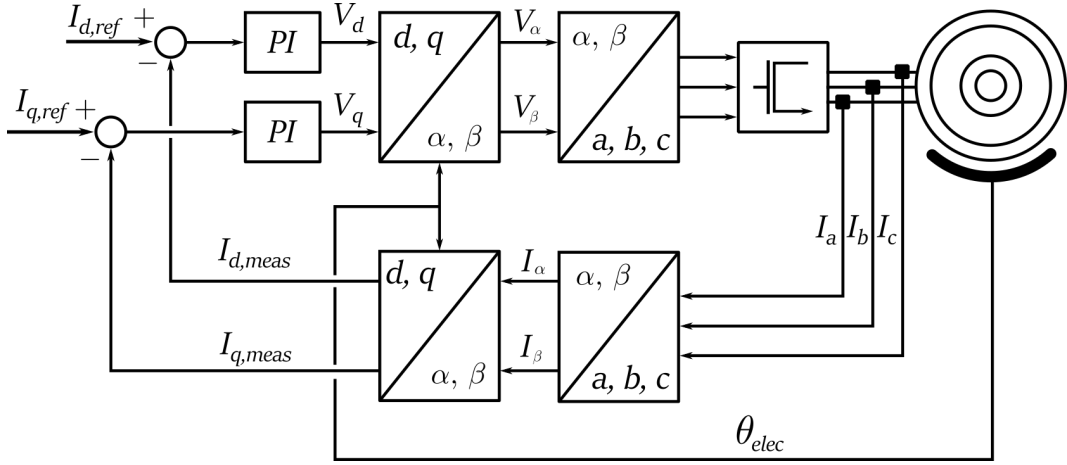


Figure 1.9: FOC Control Scheme

an interaction between direct and quadrature axes represented by terms $p\omega LI_q$ and $-p\omega LI_d$.

With new variables torque equation becomes:

$$\tau_m = pKI_q$$

and depends only on quadrature current. Regulate quadrature current so means regulate the torque generated by the motor while direct current should be regulated to 0. A different value of I_d determines, with the same torque, an increment of electrical power absorbed.

In Figure 1.9 we can see a scheme of the FOC control strategy.

[6]

Chapter 2

Estimation and Validation of parameters

2.1 Resistance and Inductance of the Motor

From previous experiments we know values of the $R_{phase}=80\text{m}\Omega$ and $L_{phase}=360\mu\text{H}$ but calculating the same values from the vedder software we obtain 2 different values: $R_{phase}=113.8\text{m}\Omega$ and $L_{phase}=79,7\mu\text{H}$ [5] [3]

To validate correct values I tried another estimation looking at the step response in the Current Loop with the motor blocked.

Considering the transfer function of the electrical part of the Motor

$$M_{el}(s) = \frac{1}{R + sL} \quad (2.1)$$

Using only a proportional controller P, as we can see in Figure 2.1 , the transfer function of the closed loop system becomes

$$F(s) = \frac{P}{P + R} \frac{1}{1 + s \frac{L}{P+R}} \quad (2.2)$$

Considering $\mu = \frac{P}{P+R}$ and $\tau = \frac{L}{P+R}$, and using $iq^*=10 \text{ A}$ and $P=0.1$

The value of the quadrature current measured at regime, as we can see in Figure

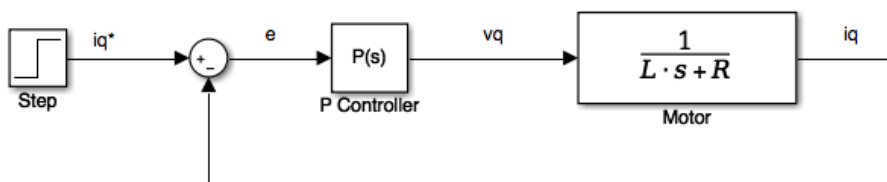


Figure 2.1: Current Loop scheme to estimate R_{phase} and L_{phase}

2.2, is more or less $i_q=3.5A$ so $\mu = 0.35$

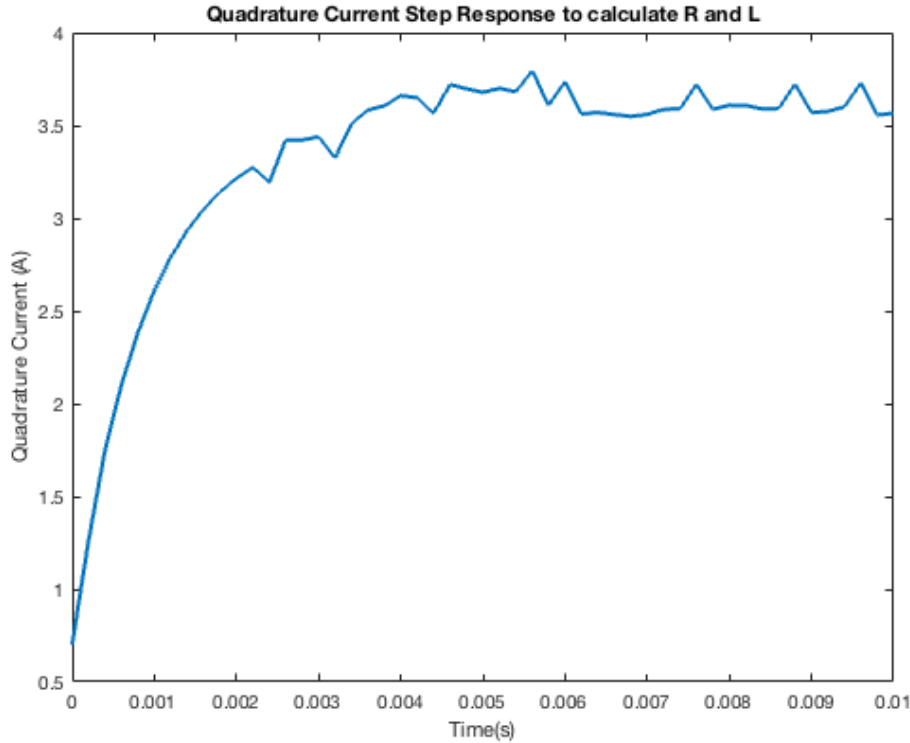


Figure 2.2: Quadrature Current Step Response to calculate R_{phase}

The time to reach regime value is around 7ms. Considering it 5τ we obtain $\tau = 1.35$.

With these values measured we can calculate $R_{phase}=186m\Omega$ and $L_{phase}=386\mu H$.

Now we have to check what is the better estimation of R_{phase} and L_{phase} . With the motor blocked we can test the step response to a reference quadrature current using a PI as a controller with the values found with the vedder software:

$$P=0.0797$$

$$I=113.8$$

The simulation is done using 3 different couple R-L found in different way

1. $R_{phase}=186m\Omega$ and $L_{phase}=386\mu H$

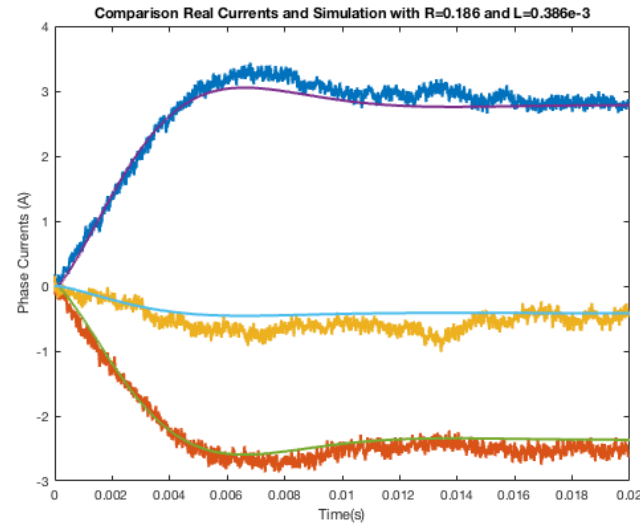


Figure 2.3: Phase Currents with $R_{phase}=186\text{m}\Omega$ and $L_{phase}=386\mu\text{H}$

2. $R_{phase}=80\text{m}\Omega$ and $L_{phase}=380\mu\text{H}$.

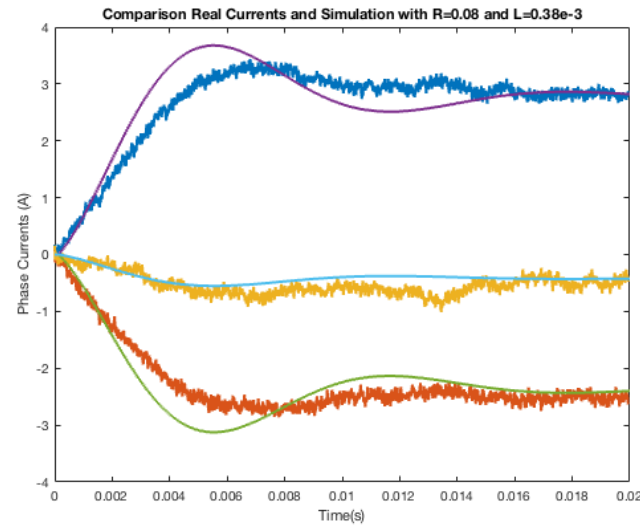


Figure 2.4: Phase Currents with $R_{phase}=80\text{m}\Omega$ and $L_{phase}=380\mu\text{H}$

3. $R_{phase}=113.8\text{m}\Omega$ and $L_{phase}=79.7\mu\text{H}$.

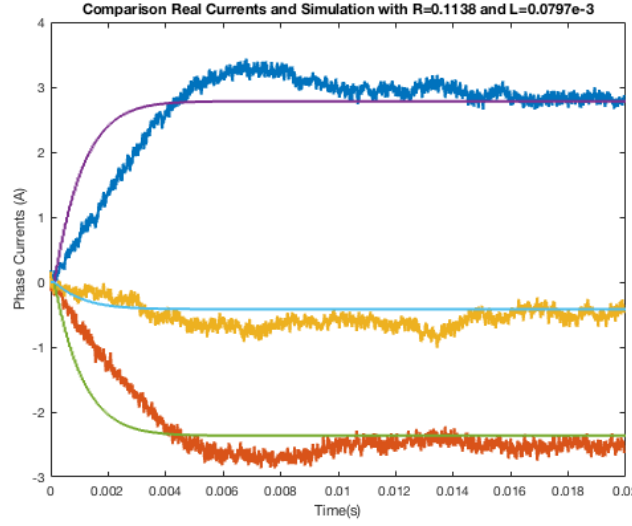


Figure 2.5: Phase Currents with $R_{phase}=113.8\text{m}\Omega$ and $L_{phase}=79.7\mu\text{H}$

In the first case, in Figure 2.3, we can see the phase currents of simulation match the currents read from real data.

Looking at real quadrature current compared with simulations we arrive at the same result as we can see in Figure

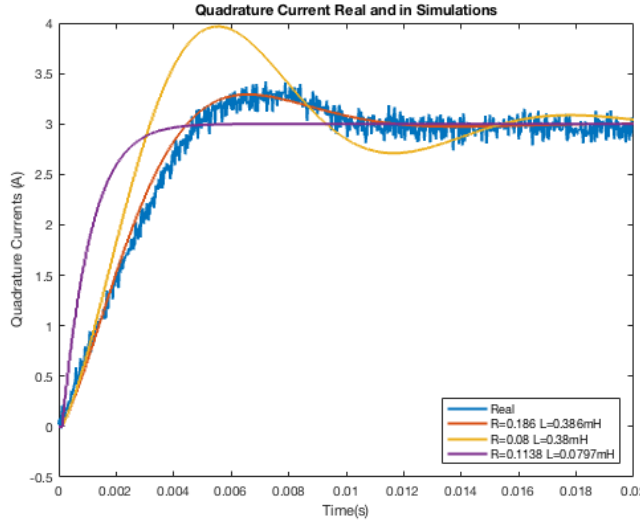


Figure 2.6: Quadrature Currents Comparison to Validate R_{phase} and L_{phase}

2.2 Flux Linkage

The flux linkage measured from the firmware is $\phi=0.029319 \text{ Wb}$ and it's comparable with the one I received from previous measurement.

2.3 Friction of the Motor

To measure the friction I use the speed control with FOC. I've imposed different values of speed, and for each value I've measured the quadrature Current at regime. Knowing the Torque constant we can calculate the Friction Torque at each speed.

From values in Table 2.1, and considering the Static Friction of 0.53 Nm, I approximated the Friction with a polynomial of 6thorder:

$$T_{Friction} = 4.51 \times 10^{-9} \omega^6 - 7.923 \times 10^{-7} \omega^5 + 5.354 \times 10^{-5} \omega^4 - 1.71 \times 10^{-3} \omega^3 + 2.64 \times 10^{-2} \omega^2 - 0.1735 \omega + 0.5278 \quad (2.3)$$

In Figure 2.7 we can see the 2.3 compared with the measured torque in Table 2.1

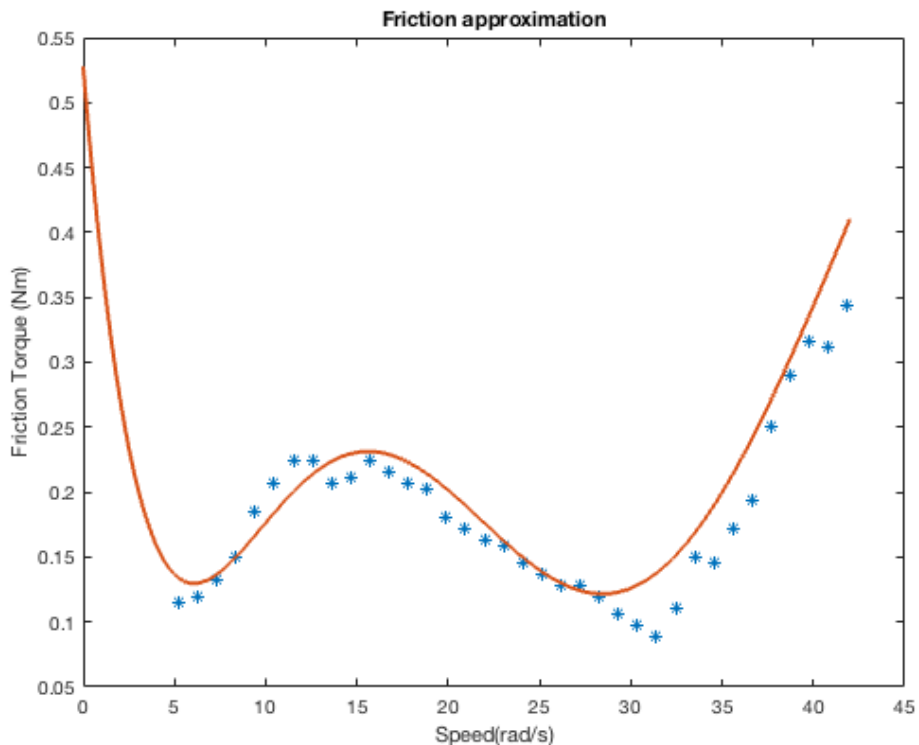


Figure 2.7: Polynomial curve that approximate the Friction of the Motor

2.4 Inertia of the Motor

The calculation of the Inertia can be done initially consider the motor a uniform disk. Knowing its weight we can calculate its Inertia J

Speed (rad/s)	Speed (RPM)	Quadrature Current (A)	Friction Torque(Nm)
5.23598776	50	0.26	0.114348
6.28318531	60	0.27	0.118746
7.33038286	70	0.30	0.13194
8.37758041	80	0.34	0.149532
9.42477796	90	0.42	0.184716
10.4719755	100	0.47	0.206706
11.5191731	110	0.51	0.224298
12.5663706	120	0.51	0.224298
13.6135682	130	0.47	0.206706
14.6607657	140	0.48	0.211104
15.7079633	150	0.51	0.224298
16.7551608	160	0.49	0.215502
17.8023584	170	0.47	0.206706
18.8495559	180	0.46	0.202308
19.8967535	190	0.41	0.180318
20.943951	200	0.39	0.171522
21.9911486	210	0.37	0.162726
23.0383461	220	0.36	0.158328
24.0855437	230	0.33	0.145134
25.1327412	240	0.31	0.136338
26.1799388	250	0.29	0.127542
27.2271363	260	0.29	0.127542
28.2743339	270	0.27	0.118746
29.3215314	280	0.24	0.105552
30.368729	290	0.22	0.096756
31.4159265	300	0.20	0.08796
32.4631241	310	0.25	0.10995
33.5103216	320	0.34	0.149532
34.5575192	330	0.33	0.145134
35.6047167	340	0.39	0.171522
36.6519143	350	0.44	0.193512
37.6991118	360	0.57	0.250686
38.7463094	370	0.66	0.290268
39.7935069	380	0.72	0.316656
40.8407045	390	0.71	0.312258
41.887902	400	0.78	0.343044

Table 2.1: Friction measured at different speed

$$J = \frac{mr^2}{2} \quad (2.4)$$

In this way J result to be $J=0.046 \text{ Kgm}^2$

But this is just a first estimation based on the uniform distribution of the mass of the motor. This is not true so to calculate the motor we can try to impose a constant Torque to have a constant acceleration and we can detect the Inertia.

We know that

$$J \frac{d\omega}{dt} = T - T_{friction} \quad (2.5)$$

So during an acceleration we can find different

$$J_i = \frac{(T - T_{friction}) \times \Delta t}{\omega_i - \omega_{i-1}} \quad (2.6)$$

And we can calculate the mean J

In 3 test with different Torque applied I found

$$J_1=0.02491 \text{ Kgm}^2$$

$$J_2=0.02182 \text{ Kgm}^2$$

$$J_3=0.02193 \text{ Kgm}^2$$

J_2 and J_3 were calculated with quadrature current of 2 and 3 Ampere respectively. The results are similar and in those cases the Friction part influenced less the measure.

The last way I used to measure the Inertia was using the same calculation but in a test in which I let the motor stop by only its friction.

With this calculation I obtained $J=0.03344 \text{ Kgm}^2$

In Figure 2.8 I compare the second test with the 3 different values found for Inertia. We can see with $J=0.02193 \text{ Kgm}^2$ the acceleration is the much closer to the real one.

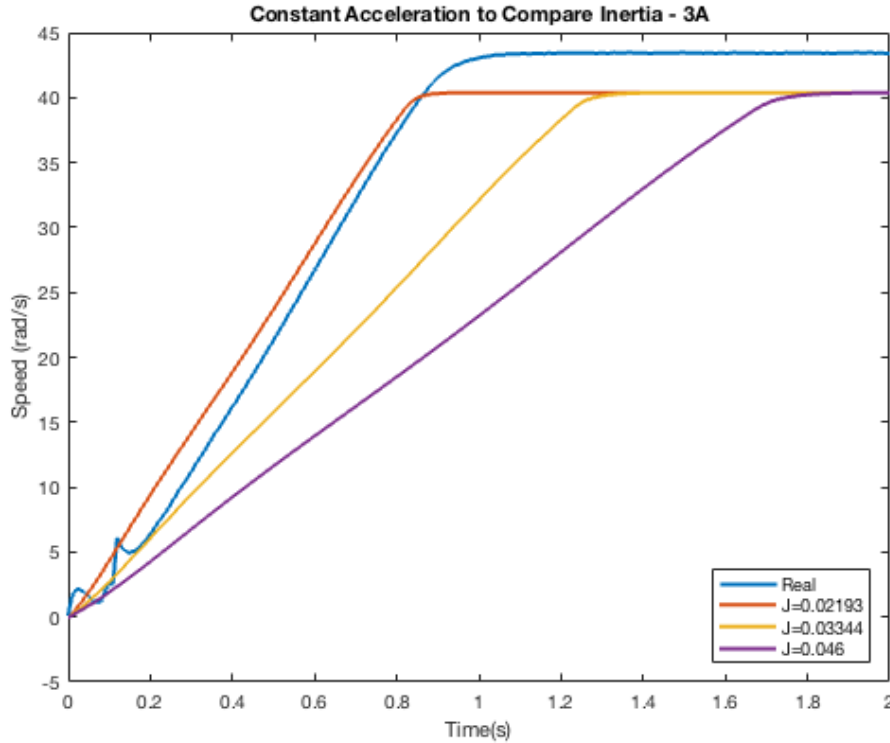


Figure 2.8: Constant Acceleration of 3 A to compare Inertia

Also changing the reference current the result is still good with $J=0.02913 \text{ Kgm}^2$ as we can see in Figure 2.9 .

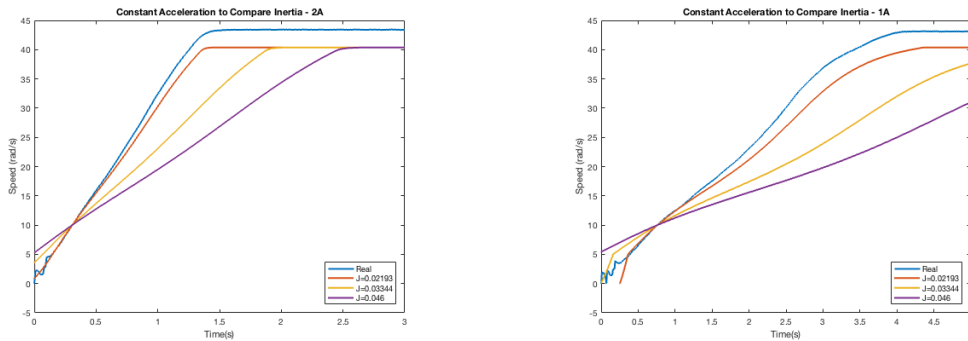


Figure 2.9: Constant Acceleration with different Current Reference

In Figure 2.10 I replicate the third test where I let the motor stopped. We can see the first part of deceleration is good approximated by $J=0.03344 \text{ Kgm}^2$ but then the better approximation is $J=0.02193 \text{ Kgm}^2$. Considering the Figure 2.7 we can see at higher speed a bit overestimation of the Friction so I consider right the Inertia $J=0.02193 \text{ Kgm}^2$

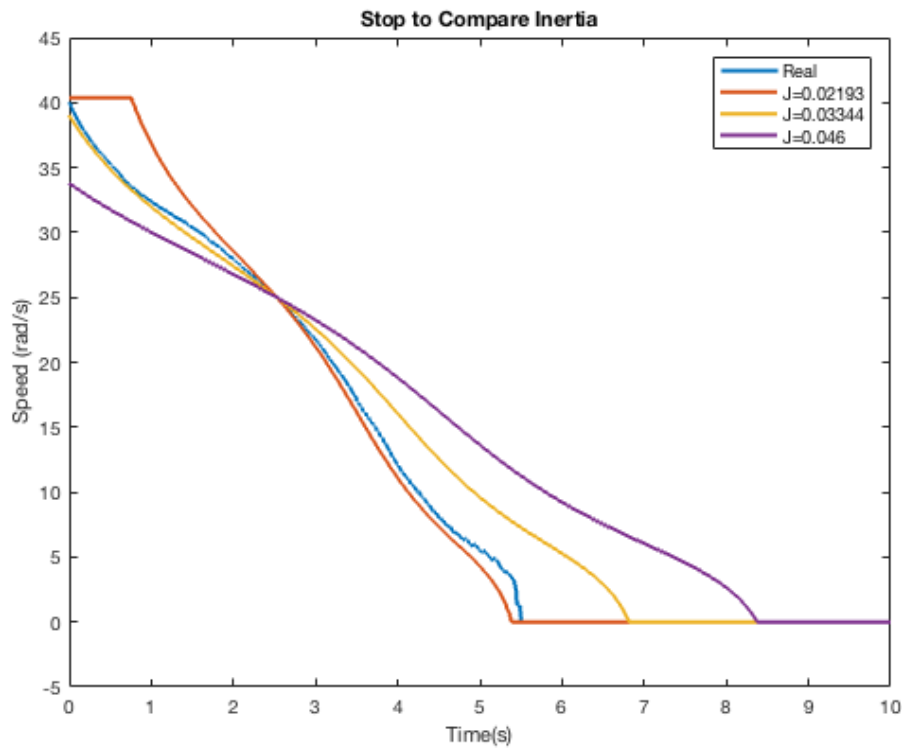


Figure 2.10: Motor stopped by Friction to compare Inertia

2.5 Parameters with Load

Introducing a load there is a variation of some mechanical proprieties in the model. In particular there will be a bigger friction and a bigger Inertia.

We can replicate the same test as before but with the load applied at the motor.

2.5.1 Friction with Load

I measured again the quadrature current at different speed and I found the friction with a polynomial approximation.

$$T_{Friction} = -2.18 \times 10^{-7}\omega^5 + 2.386 \times 10^{-5}\omega^4 - 9.131 \times 10^{-4}\omega^3 + 1.438 \times 10^{-2}\omega^2 - 0.07947\omega + 1.0995 \quad (2.7)$$

In Figure 2.11 we can see the 2.7 compared with the measured torque whit load attached

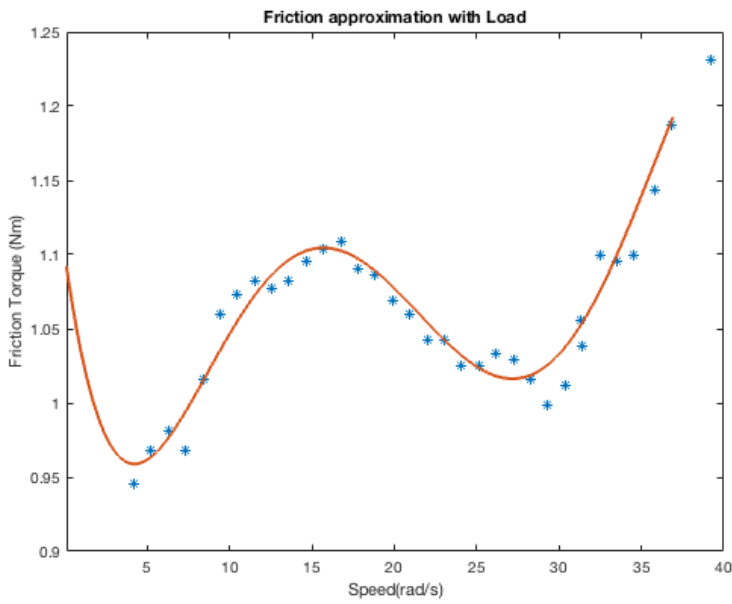


Figure 2.11: Polynomial curve that approximate the Friction of the Motor with Load

2.5.2 Inertia with Load

The inertia was calculated in the same way as before, from a constant current acceleration.

The value calculated of the inertia with load is $J=0.62517 \text{ Kgm}^2$

In Figure 2.12 we can see that the speed in simulation approximate the real speed.

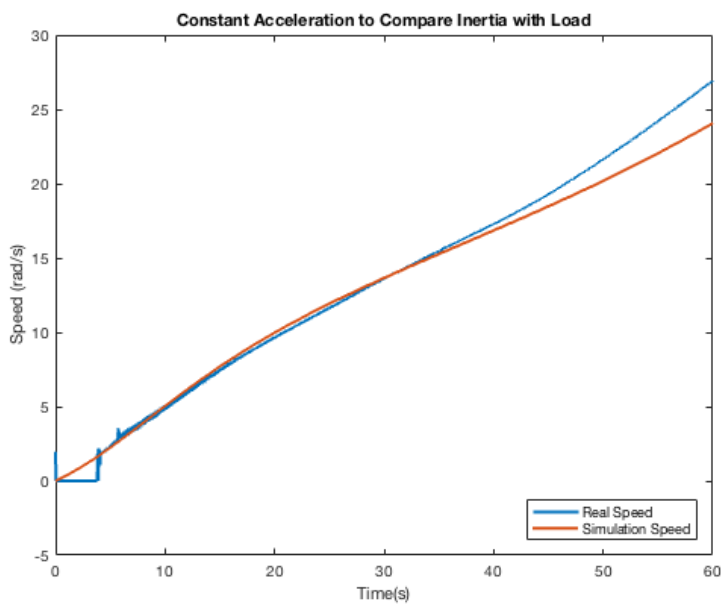


Figure 2.12: Constant Acceleration to Validate Inertia with Load

Chapter 3

Field Oriented Control Model

3.1 Simulink Model

The model in Figure 3.1 can be divided principally in 3 parts:

1. Mechanical
2. Electrical
3. Control

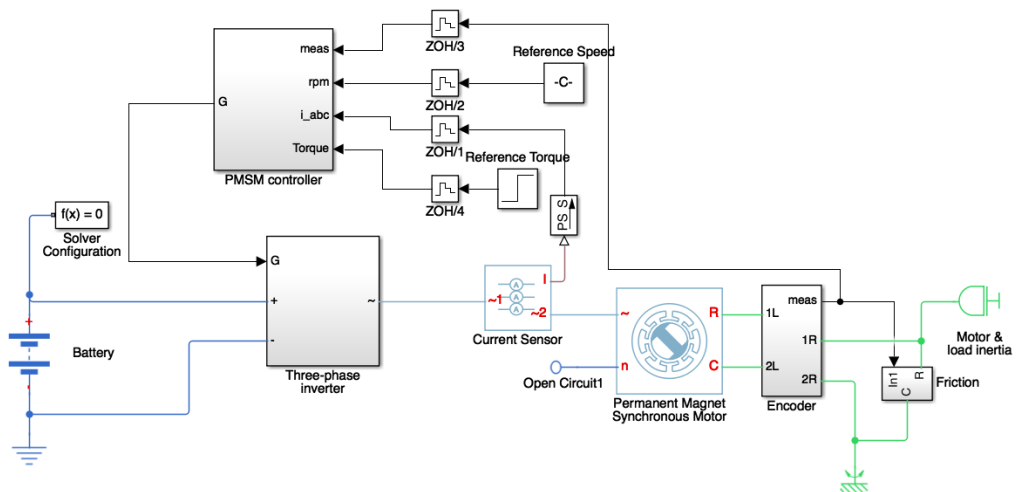


Figure 3.1: Model of the System

3.1.1 Mechanical

It is composed by the Motor, the Friction and the Motor & Load Inertia. Parameters of the motor calculated in Chapter 1 are reported in Table 3.1

3. Field Oriented Control Model

R_{phase}	186m Ω
L_{phase}	386 μH
Flux Linkage ϕ	0.029319 Wb
Number of poles N	10
Inertia J	0.02193 Kgm 2

Table 3.1: Parameters of the Motor

The friction is represented in the block shown in Figure 3.2 . In this way the Friction equation 2.3 is modify to be correct in both positive and negative direction.

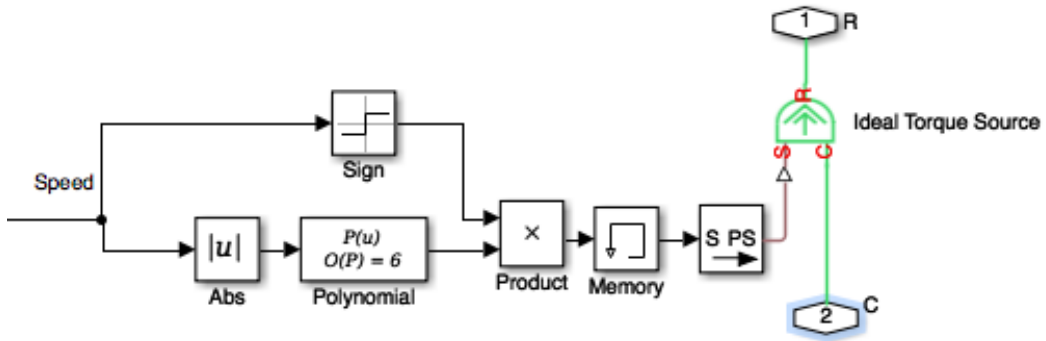


Figure 3.2: Friction Model

3.1.2 Electrical

It is composed by the Battery, and the Three-Phases Inverter.

In Figure 3.3 we can see the model of the Inverter

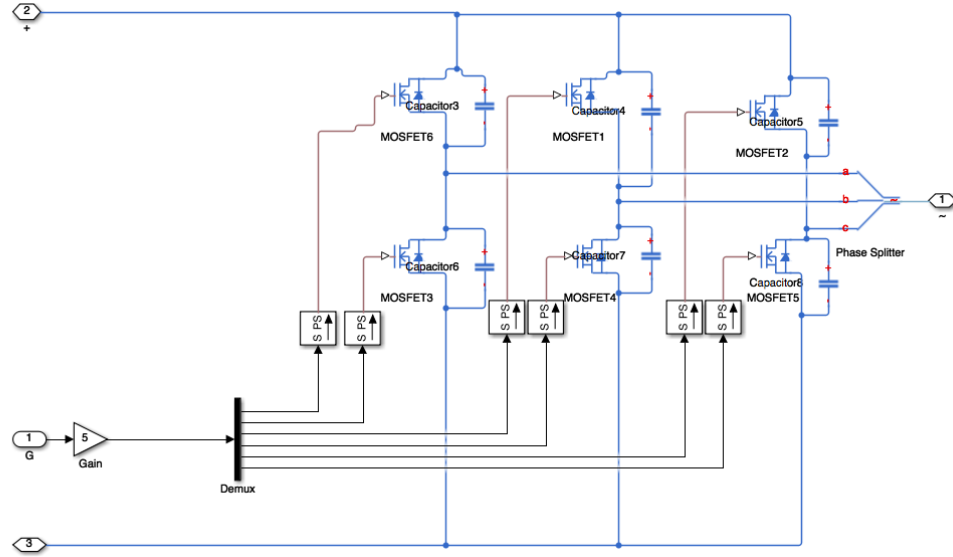


Figure 3.3: Model of Inverter

Six signals G , arriving from the controller, control the gates of the 6 MOSFETs as 6 switches.

3.1.3 Control

The control represents the code of the microcontroller. It includes both the Feedback Controller and the PWM Generator as we can see in Figure 3.4 .

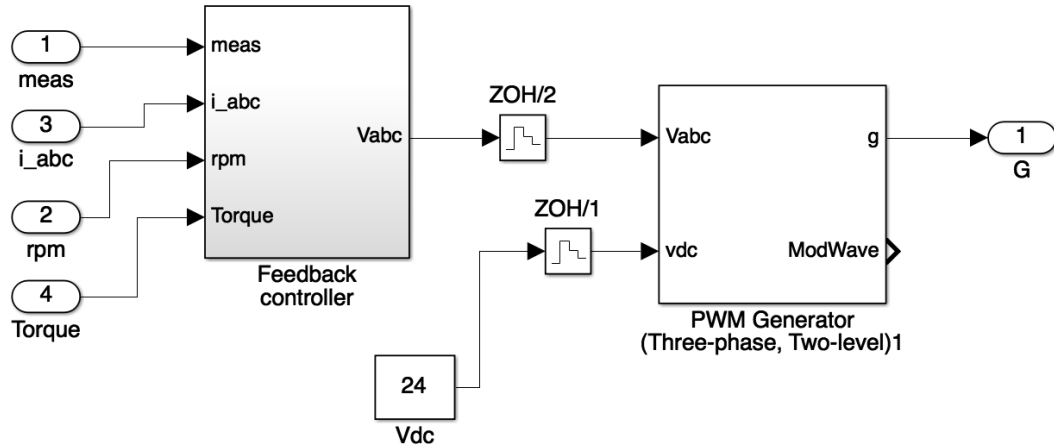


Figure 3.4: Model of Controller

The Feedback Controller, shown Figure 3.5 , in include the Speed Loop and the Current Loop. It is possible decide to use only one or both through a switch.

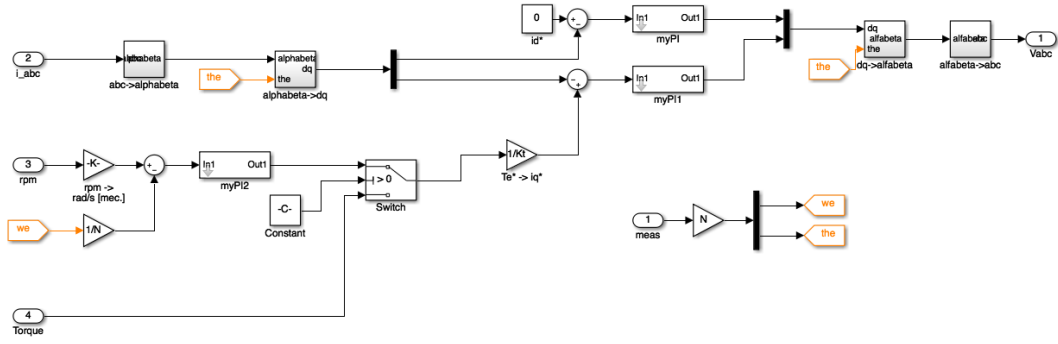


Figure 3.5: FOC and Speed Controller

The generation of PWM is made by a block which permit to have a Space Vector Modulation having as input the medium voltage we have as a target.

3.2 Simplified Model

To increase the speed of simulations I also used a simplified model. In this model shown in Figure 3.6 the electrical part of the motor is represented using directly the medium voltage.

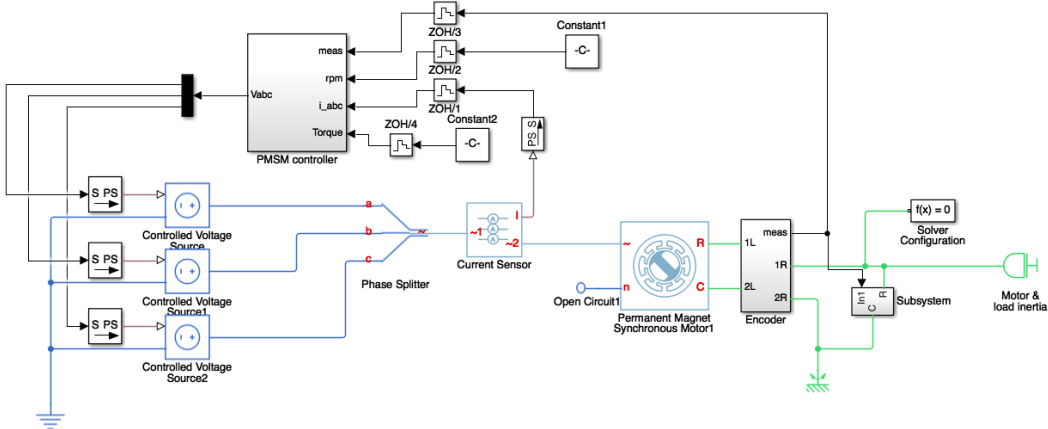


Figure 3.6: Model of the System Simplified

Also the Controller is modified to have the voltages as output instead the gate signal.

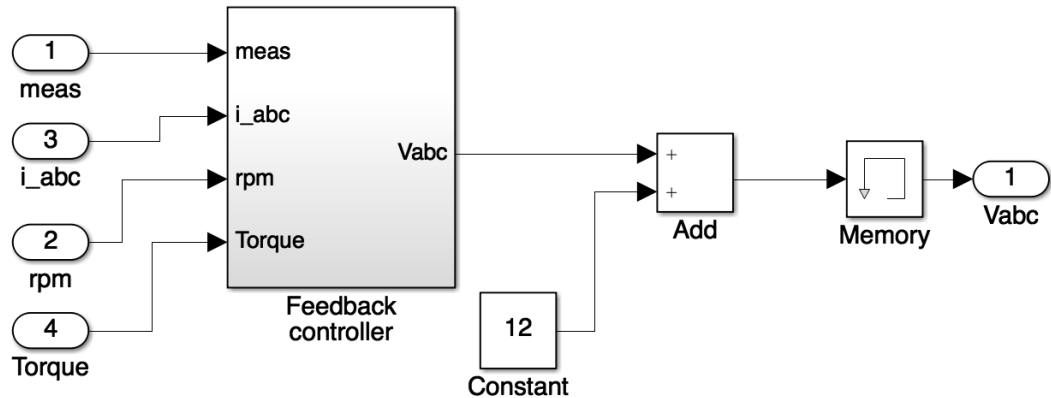


Figure 3.7: Model of Controller Simplified

With both models I tried simulations with the same input, expecting the same output. In Figure 3.8 we can see the comparison. Under the red lines there are blue lines superimposed. The main difference is in the quadrature current: in the complete model there are a lot of oscillation because of the effect of the inverter while there aren't oscillation in the simplified one.

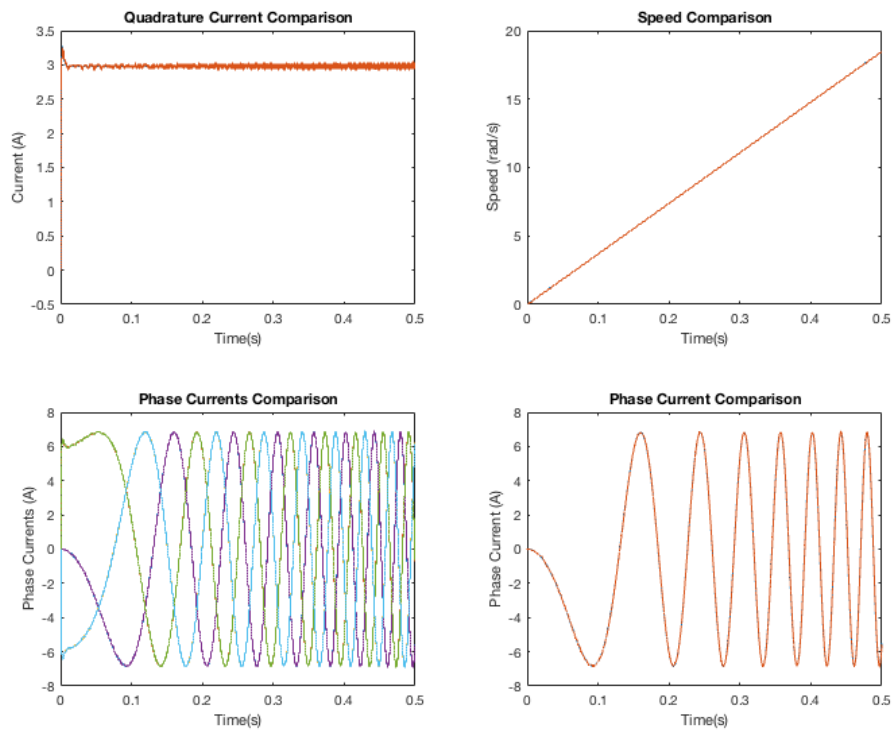


Figure 3.8: Comparison between complete and simplified models

3.3 Validation of the Model

To validate the model tests in various condition was made with the real motor and then on simulation.

1. Current Control

- (a) Step Response - Current with motor Blocked
- (b) Step Response - Speed Variaton
- (c) Regime Current

2. Speed Control

- (a) Step Response - Speed Variation

Step Response - Speed Variation

This test consists in measure the phase currents with the motor Blocked. In Figure 3.9 we can see that simulation currents are less noisy but they follow good real data.

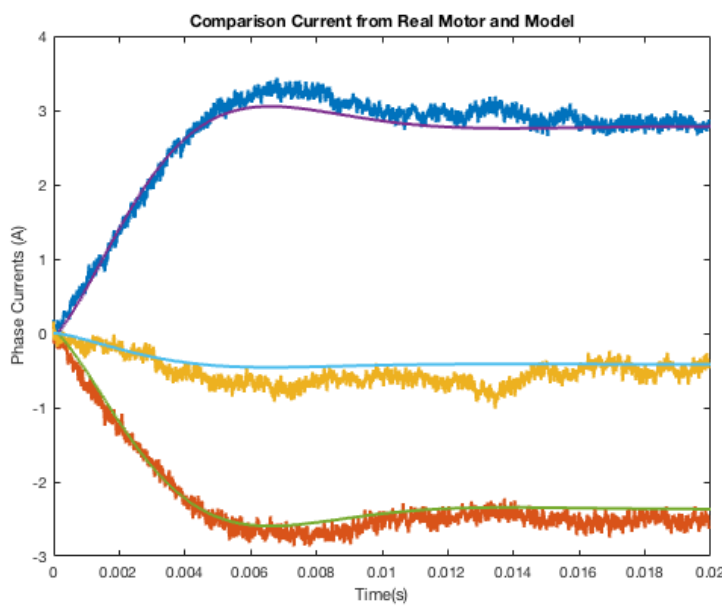


Figure 3.9: Phase currents step response to quadrature current reference

If we look also to the quadrature Current in Figure 3.10 we can see the good approximation of the Simulation respect the real Motor.

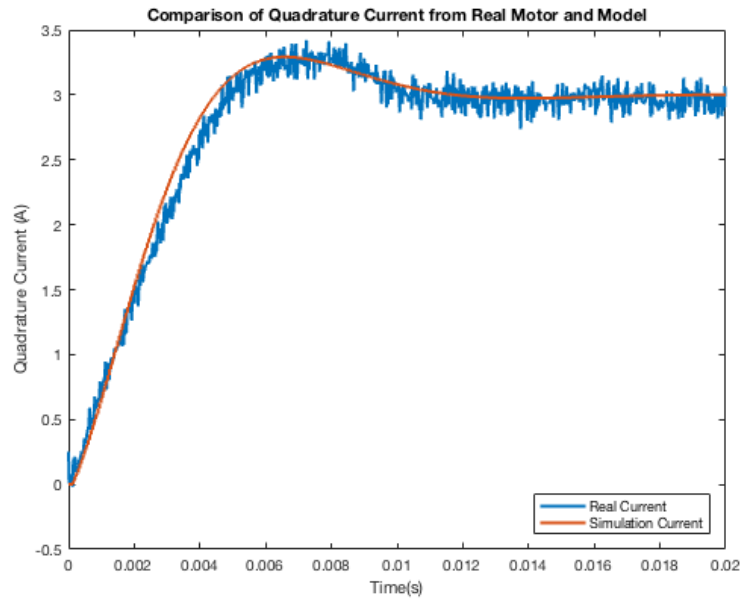


Figure 3.10: Quadrature current step response to current reference

Step Response - Speed Variation

In this test the Motor is being unblocked and we can see its speed when we impose a quadrature current as a reference. In Figures 3.11 , 3.23 and 3.13 we can see the differnt comparison with I_q reference respectively of 1A, 2A and 3A.

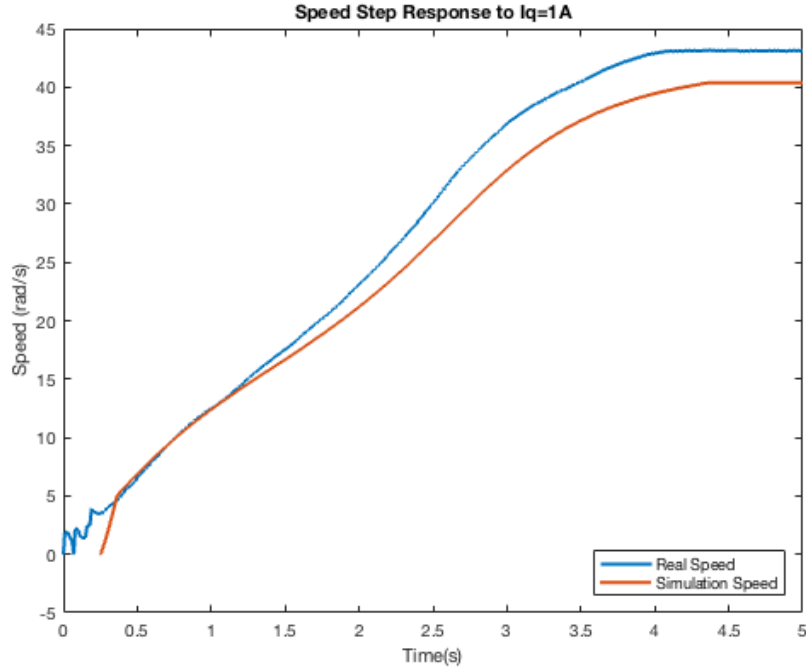


Figure 3.11: Speed step response to current reference 1A

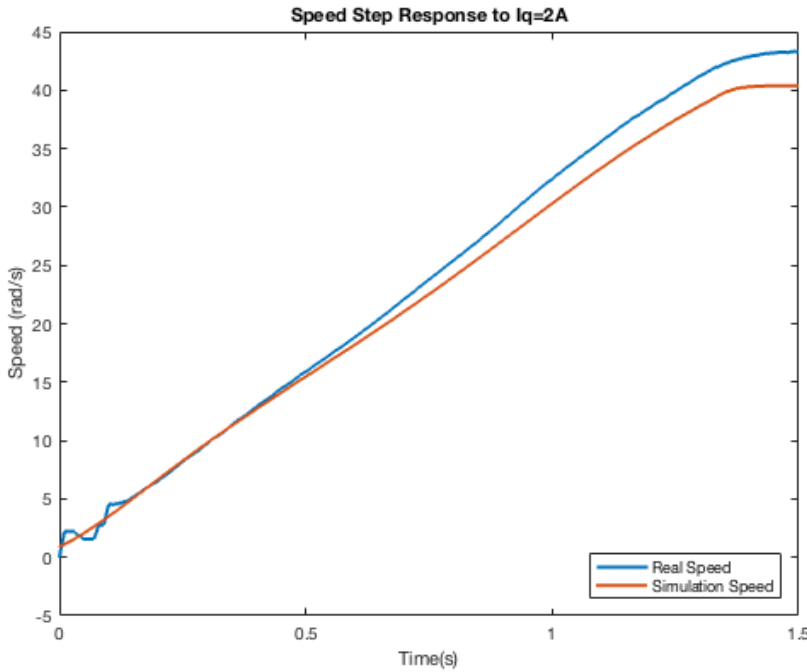


Figure 3.12: Speed step response to current reference 2A

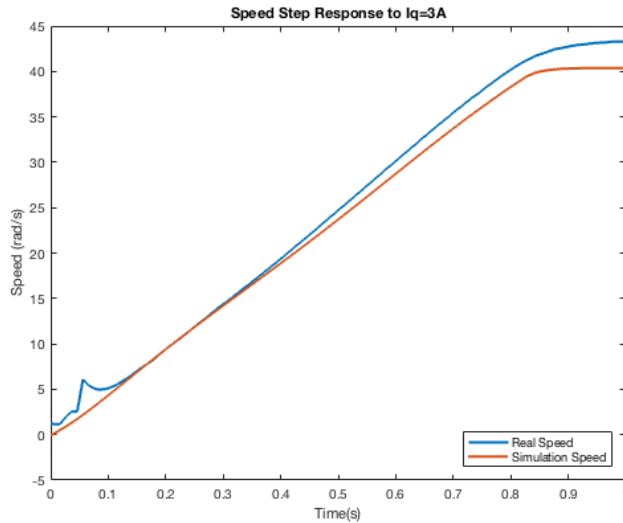


Figure 3.13: Speed step response to current reference 3A

The main problem of the simulation is caused by the maximum speed reached, it depends directly on the voltage applied by batteries. In simulation I considered the Voltage always to be of Volts. Furthermore simplifying the model, skipping the Space Vector Modulation, we can have smaller variation on the voltage applied when it is closed to the maximum value.

The same test done also with the load attached has the same result, as we can

see in Figure 3.14

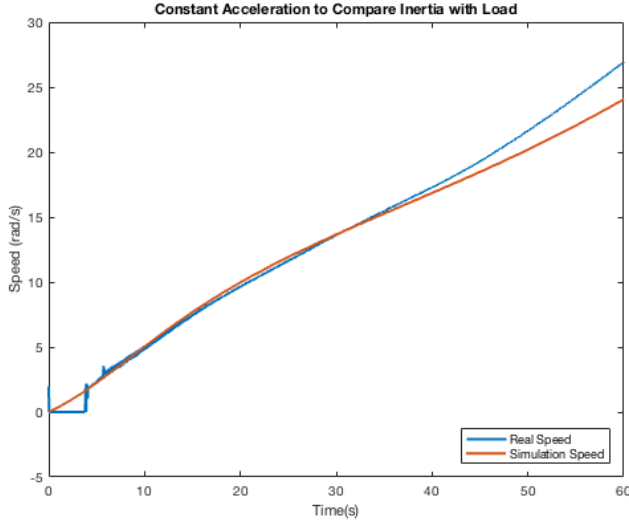


Figure 3.14: Speed step response to current reference 3A with Load

Regime Current

In this test we can see the phase current in the motor while it is moving at constant speed, reached imposing a quadrature current.

In Figure 3.15 we can see phase current compared. The current in simulation is a perfect sine curve, while the Real current is a bit different with some peak. However the simulation is a good approximation of the real current.

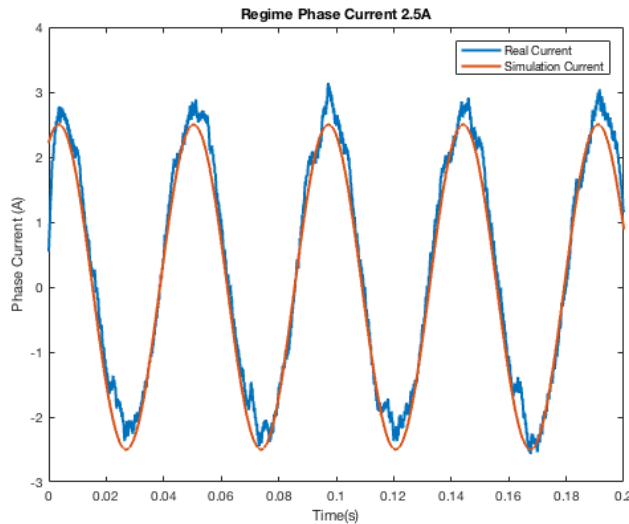


Figure 3.15: Regime phase current with $i_q=2.5A$

In Figure 3.16 we can compare the three-phase currents. The results are the same

3. Field Oriented Control Model

as before.

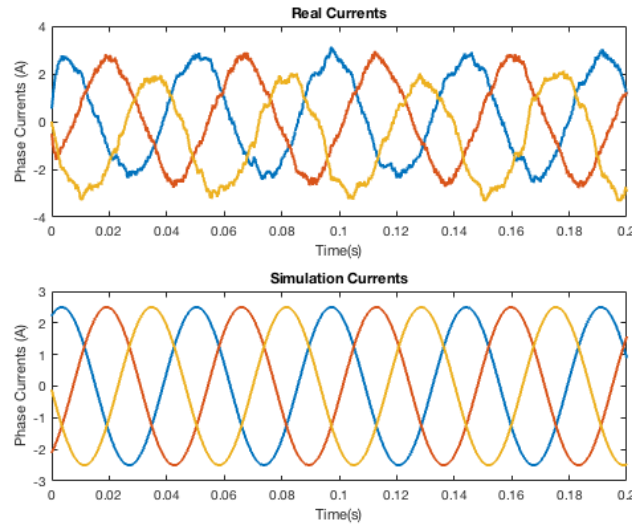


Figure 3.16: Regime phase currents with $i_q=2.5A$

Using different quadrature current as reference has the same result as we can see in Figure 3.17 and 3.18

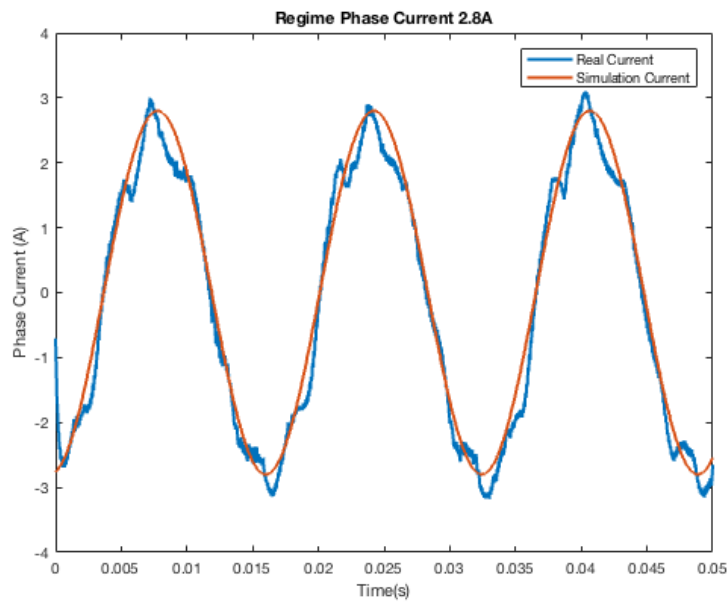


Figure 3.17: Regime phase current with $i_q=2.8A$

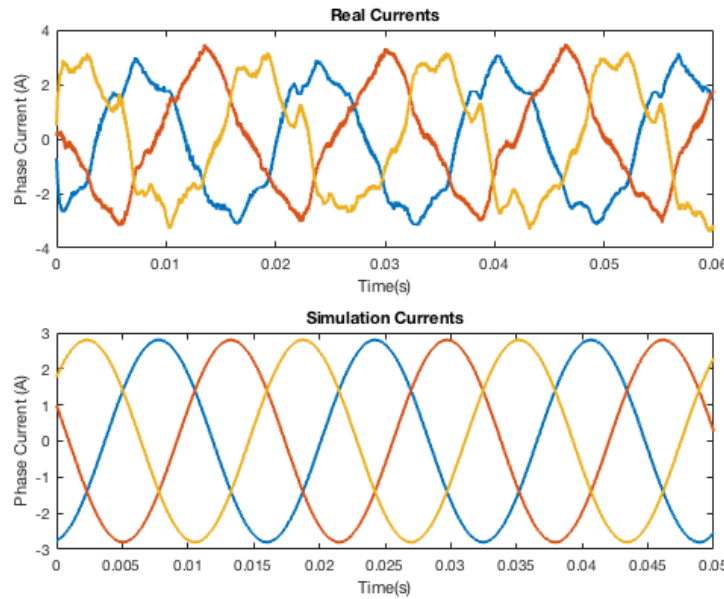


Figure 3.18: Regime phase currents with $i_q=2.8A$

These results were obtained with the load attached to the motor. Without the load the not ideal part of the motor becomes more significant and it is more difficult to see the sine behavior of the current.

Step Response - Speed Variation

In this test we compared the speed of the motor using also the Speed Loop and not only the Current Loop.

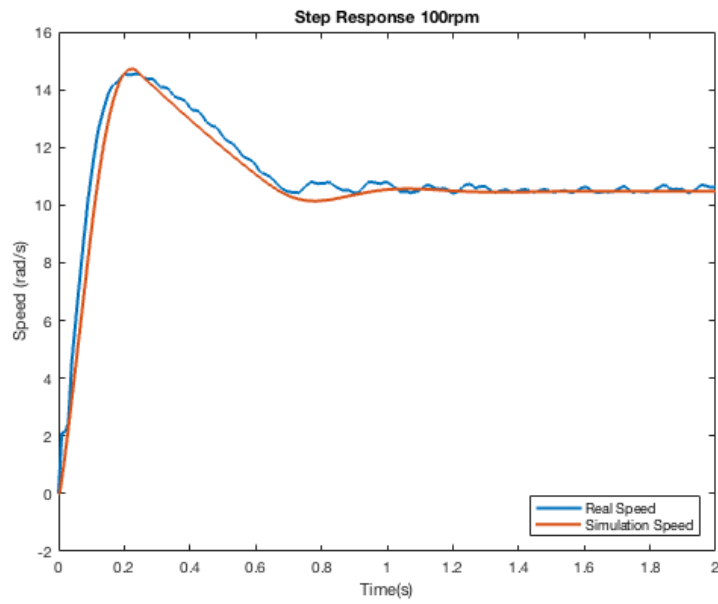


Figure 3.19: Step Response 100 rpm

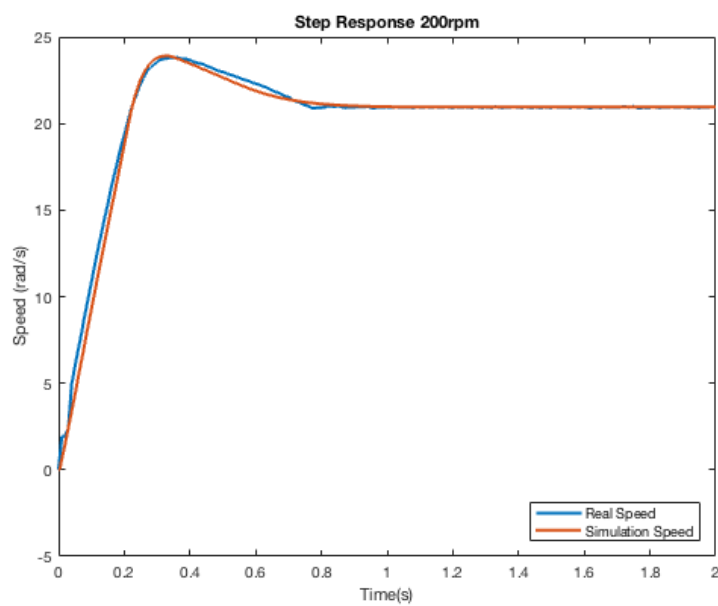


Figure 3.20: Step Response 200 rpm

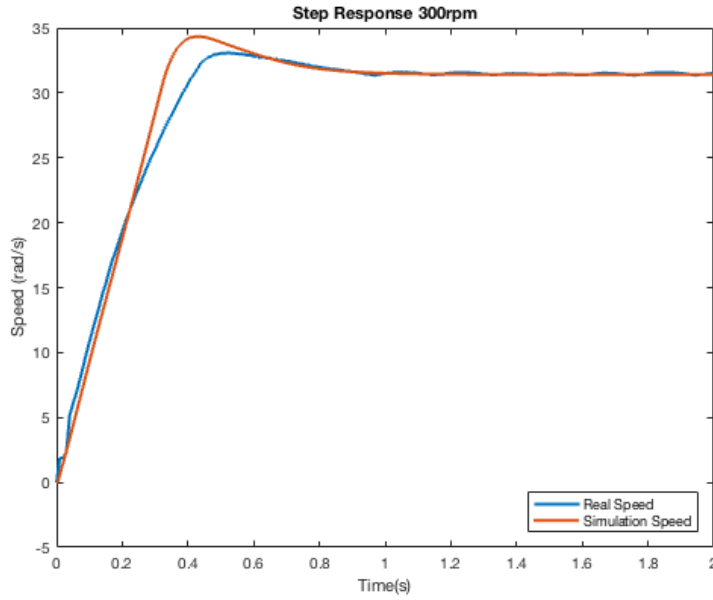


Figure 3.21: Step Response 300 rpm

The simulation speed is a good approximation of the real speed in both Figure 3.19, 3.20 and 3.21. However in Figure 3.21 there is some problem caused by limitation of the current, not completely considered in simulation, when the speed increase.

3.4 Controller Parameters

The model can be now considered an approximation of the real motor, so now we have to find the best parameters to control the motor.

3.4.1 Current Loop

The electrical transfer function of the Motor is

$$M_{el} = \frac{1}{R + sL} \quad (3.1)$$

We can control it in with a PI control in closed Loop, the transfer function (in open loop) will be

$$L(s) = \frac{sP + I}{s} \frac{1}{R + sL} \quad (3.2)$$

The first approach we can use is to tune P and I to cancel the pole. This transfer function can be seen as

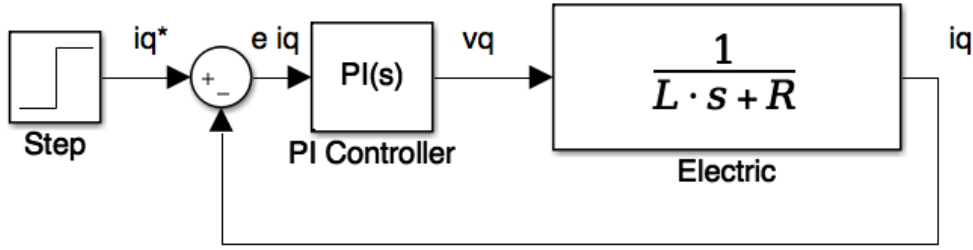


Figure 3.22: Current control loop

$$L(s) = \frac{P}{L} \frac{s + \frac{I}{P}}{s + \frac{R}{L}} \quad (3.3)$$

So if $\frac{I}{P} = \frac{R}{L}$ the pole and the zero will be cancelled the function will become

$$L(s) = \frac{P}{L} \frac{1}{s} \quad (3.4)$$

Choosing $\omega_0=1000$ rad/s, more than a decade less than the switching frequency of the mosfet fsw=10kHz we obtain

$P=0.23$ and $I=186$

Another way to calculate parameters of PI is calculating the transfer function of the closed loop:

$$F(s) = \frac{P}{L} \frac{s + \frac{I}{P}}{s^2 + \frac{P+R}{L}s + \frac{I}{L}} \quad (3.5)$$

Considering only the denominator we can see it as

$$s^2 + 2\xi\omega_0 s + \omega_0^2$$

Using $\omega_0=1000$ rad/s as before and $\xi=1$ (coincident real poles) we will have

$$P = 0.274$$

and

$$I = 230$$

Instead with $\xi=1/\sqrt{2}$ we will obtain

$$P = 0.139$$

and

$$I = 230$$

In the Figure 3.23 we can see the difference using these values of parameters

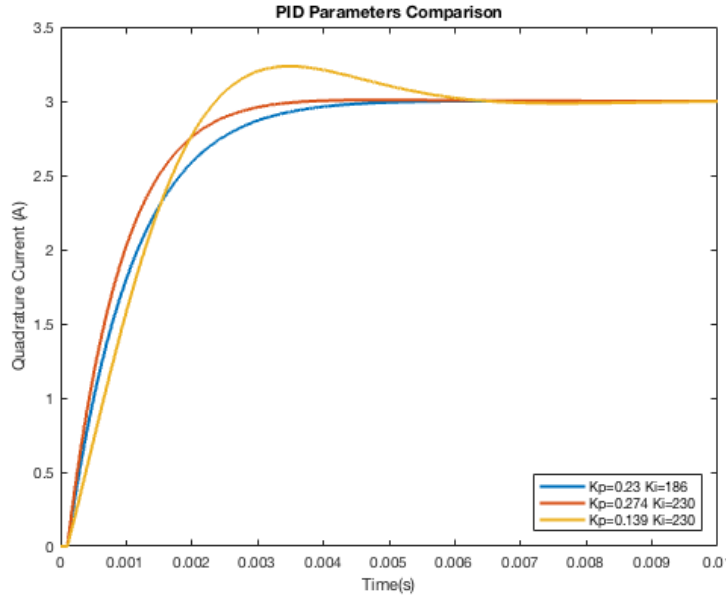


Figure 3.23: Step Response of quadrature current with different P and I values

3.4.2 Speed Loop

The mechanical transfer function of the motor, not considering friction, is

$$M_{mec}(s) = \frac{1}{J \cdot s} \quad (3.6)$$

The friction coefficient can be omitted in calculation because it helps in having stability, so if we have a stable system without it, the system with it will be stable.

The structure of the control is composed by two nested loop: the Current Loop calculated before is inside the Speed Loop as we can see in Figure 3.24 .

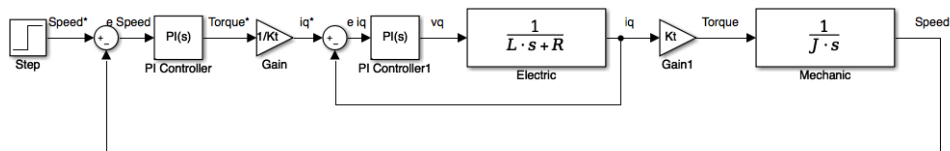


Figure 3.24: Speed and Current Loop Nested

If we consider the Current Loop enough fast, so the Bandwidth of Current Control is higher than the Bandwidth of Speed Control, we can consider the simplified model of the Speed Loop shown in Figure 3.25 .

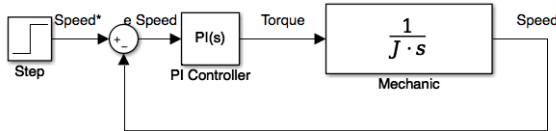


Figure 3.25: Speed and Current Loop Nested

We can't cancel pole introducing a zero, so we will calculate the closed loop function and we will find parameters from denominator, as we have done in the control loop.

The closed loop transfer function will be

$$F(s) = \frac{P}{J} \frac{s + \frac{I}{P}}{s^2 + \frac{p}{J}s + \frac{I}{J}} \quad (3.7)$$

Using $\omega_0=100$ rad/s, 1 decade less than ω_0 of current loop, and $\xi=1$ we will have

$$P = 4.386$$

and

$$I = 219.3$$

Instead with $\xi=1/\sqrt{2}$ we will obtain

$$P = 3.101$$

and

$$I = 219.3$$

In Figure 3.26 we can see the difference using these values of parameters.

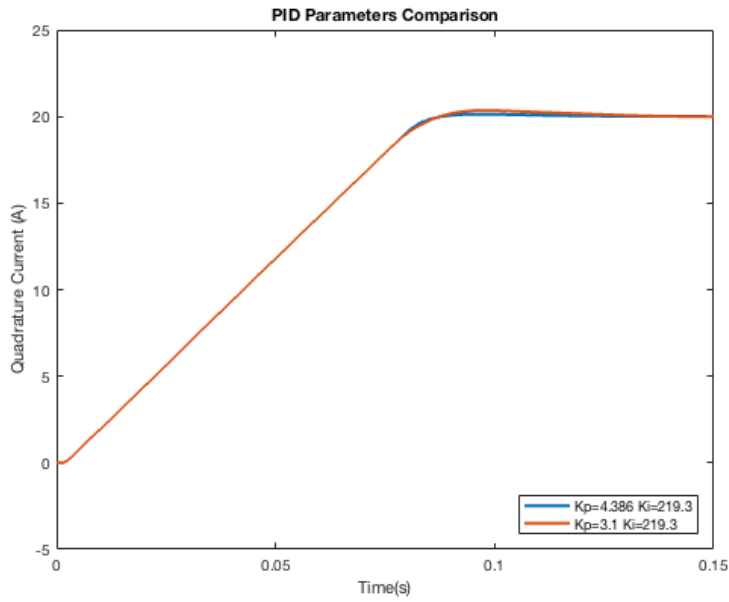


Figure 3.26: Speed Step Response

Looking better on the peak in Figure we can see there isn't an improvement choosing $\xi=1/\sqrt{2}$

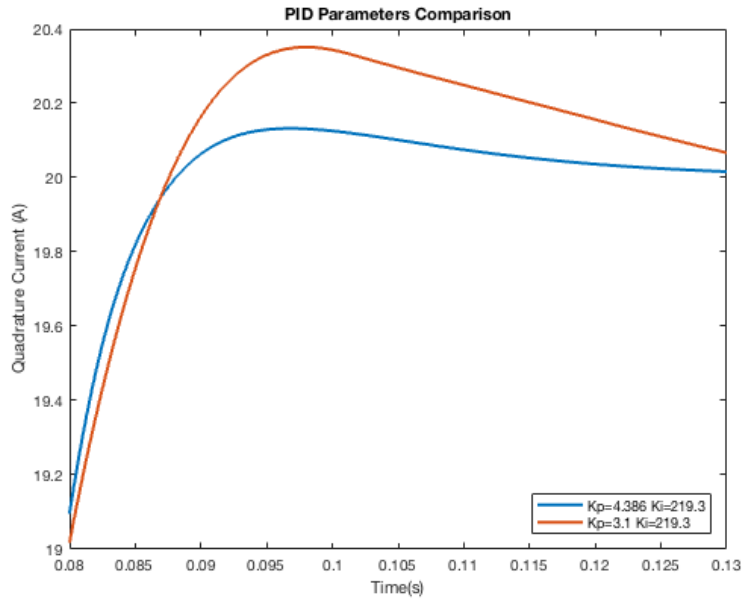


Figure 3.27: Speed Step Response

Chapter 4

Brushless DC Control Model

4.1 Simulink Model

The model in Figure 4.1 is very similar to the FOC Model: Electrical and Mechanical part are exactly the same, the difference is about the controller. Now the motor is considered a BLDC motor, so we consider the BEMF as trapezoidal.

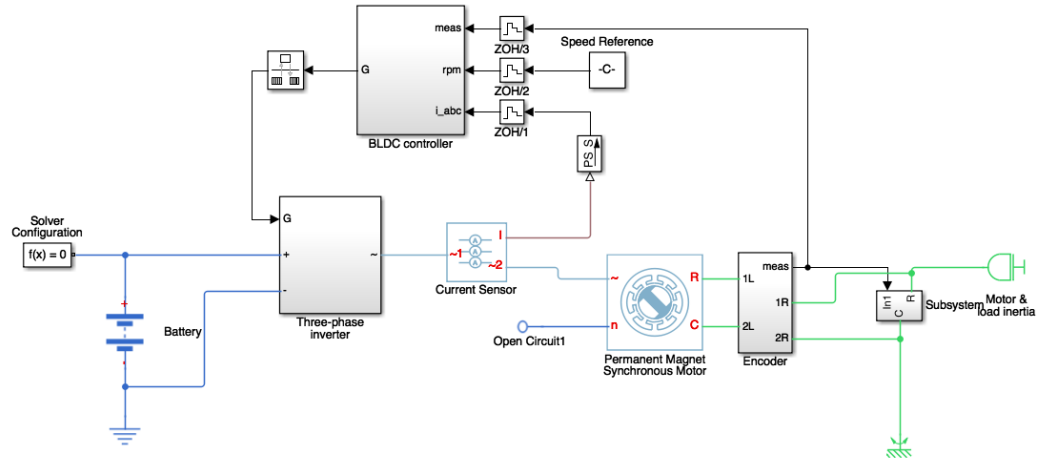


Figure 4.1: Model of the System

4.1.1 Control

The main part of the control in Figure 4.2 is similar to the FOC model with a Feedback Controller and a PWM generator. Now we have also 2 other blocks, one who permit to calculate the output of the Hall Effect Sensor and the other one to calculate what phase we are going to excite.

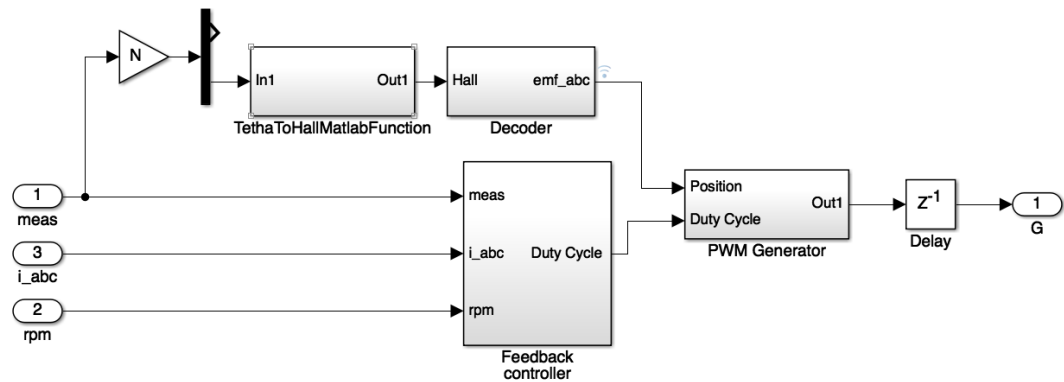


Figure 4.2: Model of Controller

The simplest feedback controller is just made by a PI controller in the speed loop as we can see in Figure 4.3 .

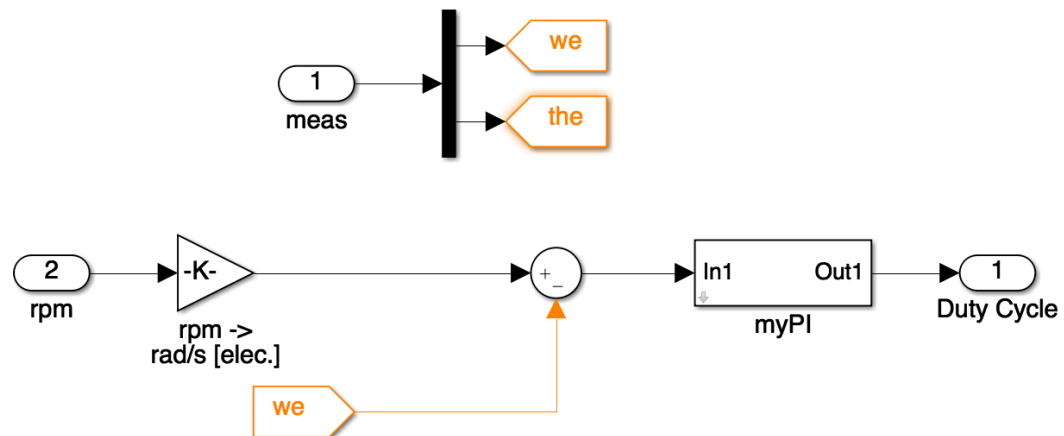


Figure 4.3: Speed Control BLDC

In Figure 4.4 is shown another way to implement the controller, taking care about the current. In this way we have also a current loop inside the Speed Loop.

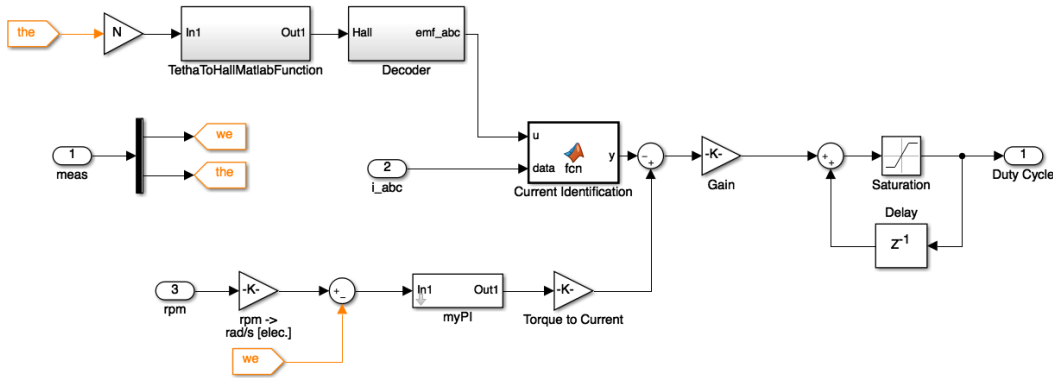


Figure 4.4: Speed Control BLDC with Current Loop

4.2 Simplified Model

Also with the BLDC Model To increase the speed of simulations I used a simplified model. In the model in Figure 4.5 I represent the electrical part of the motor using directly the medium voltage.

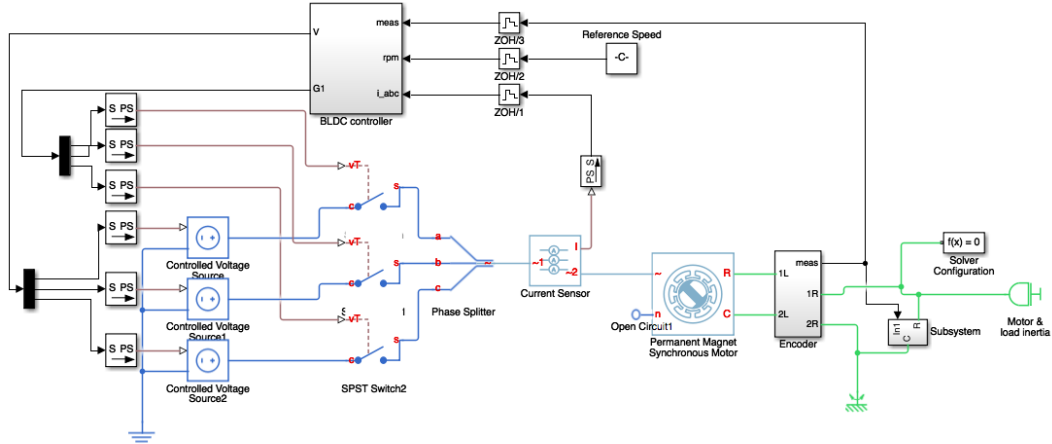


Figure 4.5: Model of the System Simplified

In this case the generation of the voltage is a little bit tricky because there is always one of the 3 phases held disconnected. I used 3 switches to connect and disconnect phases with voltage generators.

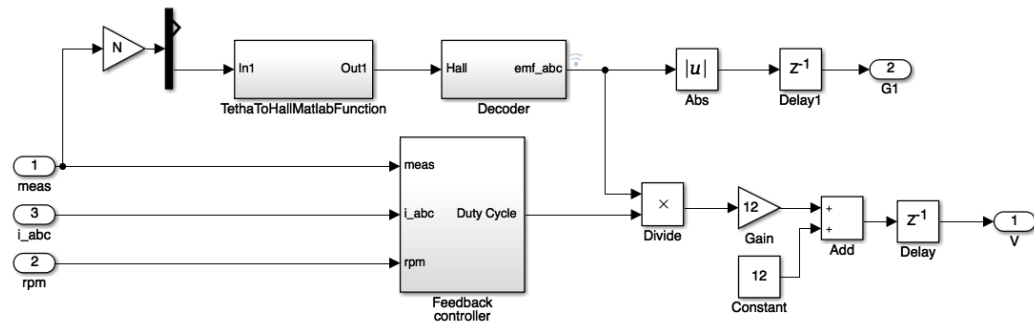


Figure 4.6: Model of Controller Simplified

Simplifying the model the pwm generator disappear and I just do some calculation to impose the medium voltage as seen in Figure 4.6 .

4.3 Validation of the Model

To validate the model tests in various condition was made with the real motor and then on simulation.

1. Duty Cycle Reference

(a) Without Load

- i. D = 10%
- ii. D = 50%
- iii. D = 90%

(b) With Load

- i. D = 10%
- ii. D = 50%

2. Speed Reference at Regime

(a) Without Load

- i. Speed = 100 rpm
- ii. Speed = 200 rpm
- iii. Speed = 400 rpm

(b) With Load

- i. Speed = 100 rpm
- ii. Speed = 200 rpm

3. Speed Reference - Step Response

(a) Without Load

- i. Speed = 100 rpm
- ii. Speed = 200 rpm

1. Duty Cycle Reference

In following tests we impose a Duty Cycle and we look at currents and voltages to compare simulation and experimental data both with and without load

a. Without Load

$$D = 10\%$$

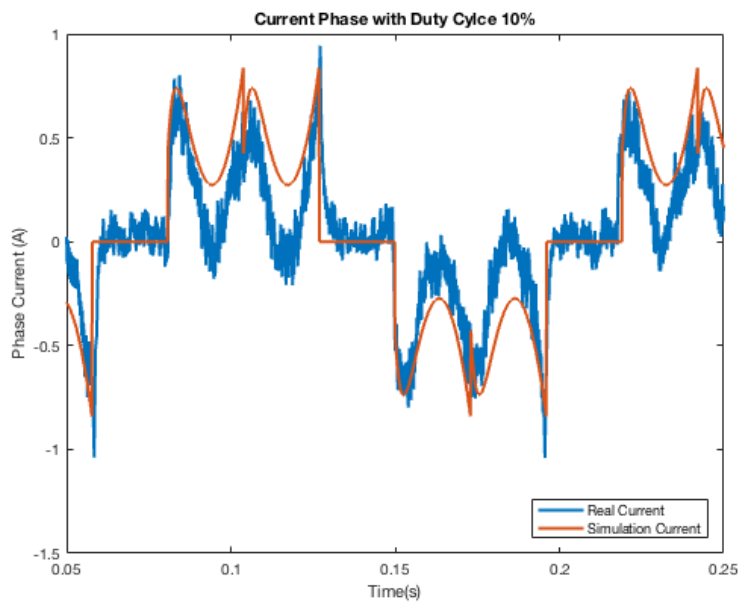


Figure 4.7: Current Phase with Duty Cycle 10%

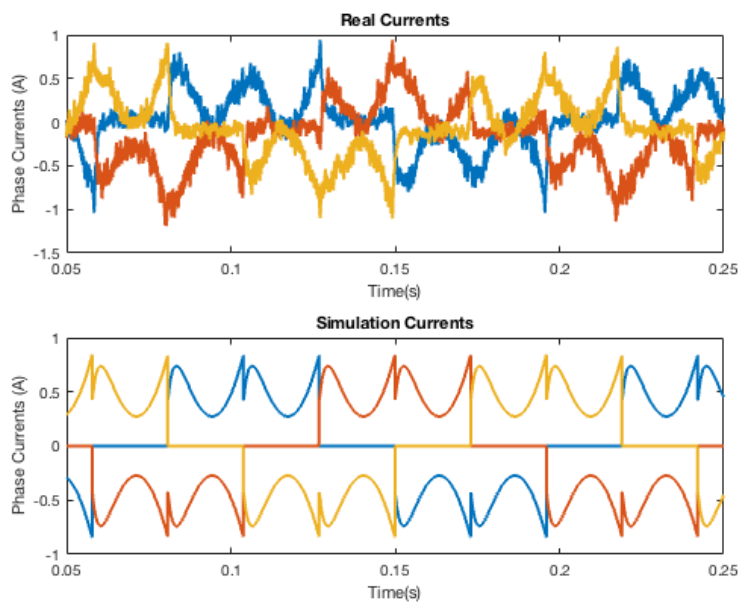


Figure 4.8: Comparison Current Phases with Duty Cycle 10%

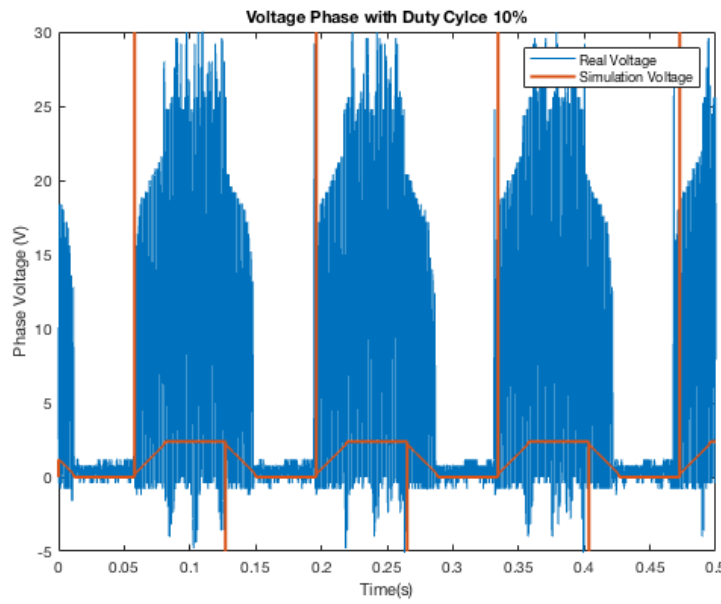


Figure 4.9: Voltage Phase with Duty Cycle 10%

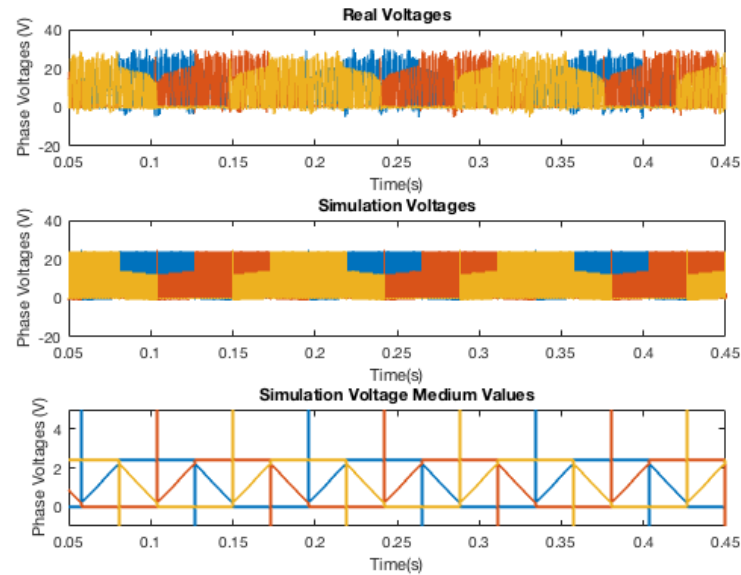


Figure 4.10: Comparison of Voltage Phases with Duty Cycle 10%

4. Brushless DC Control Model

$D = 50\%$

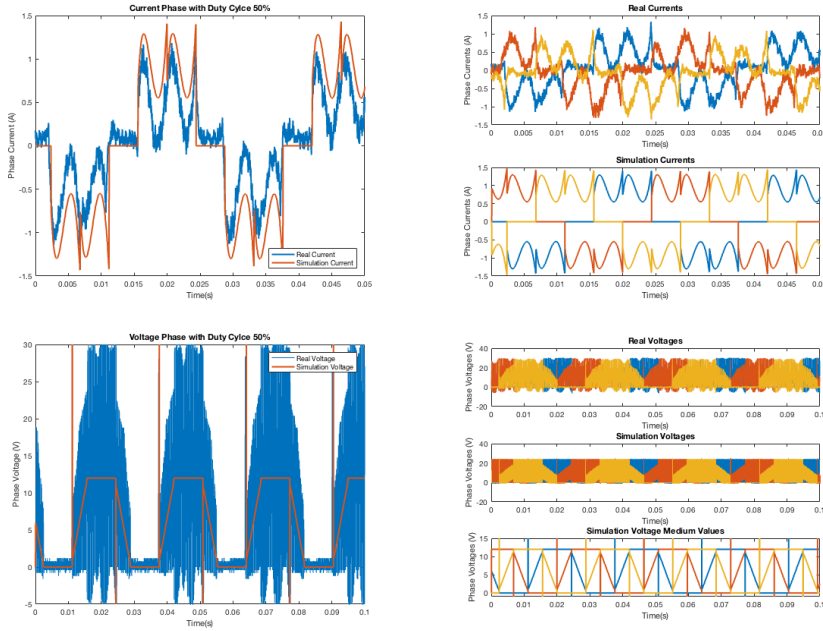


Figure 4.11: Tests with Duty Cycle 50%

$D = 90\%$

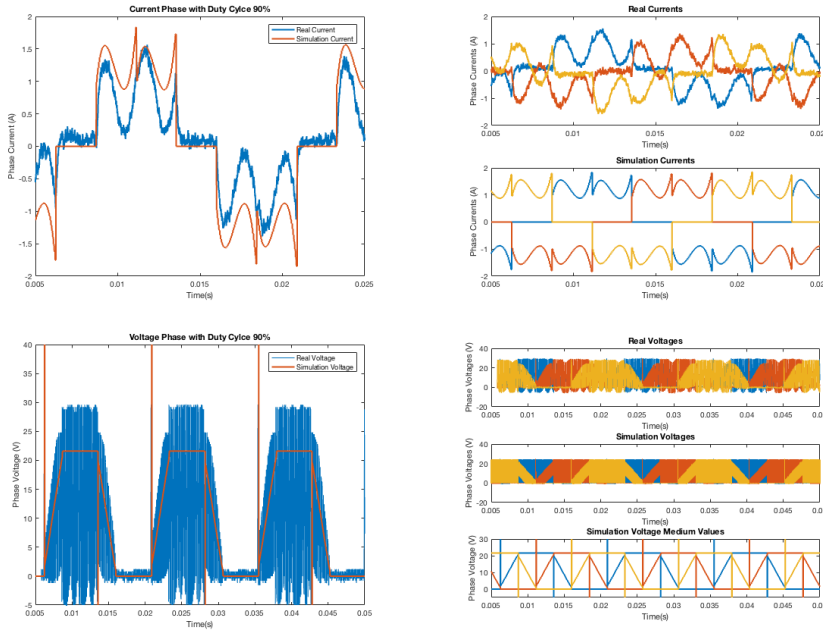


Figure 4.12: Tests with Duty Cycle 90%

b. With Load

$D = 10\%$

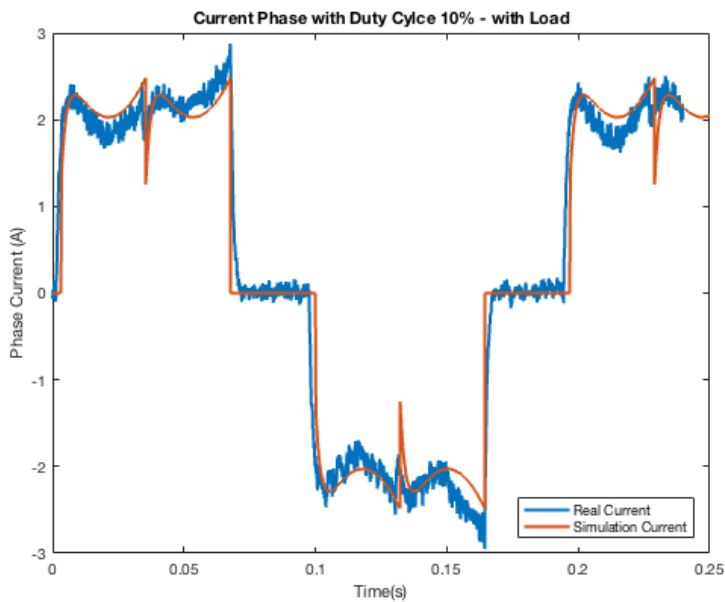


Figure 4.13: Current Phase with Duty Cycle 10% - With Load

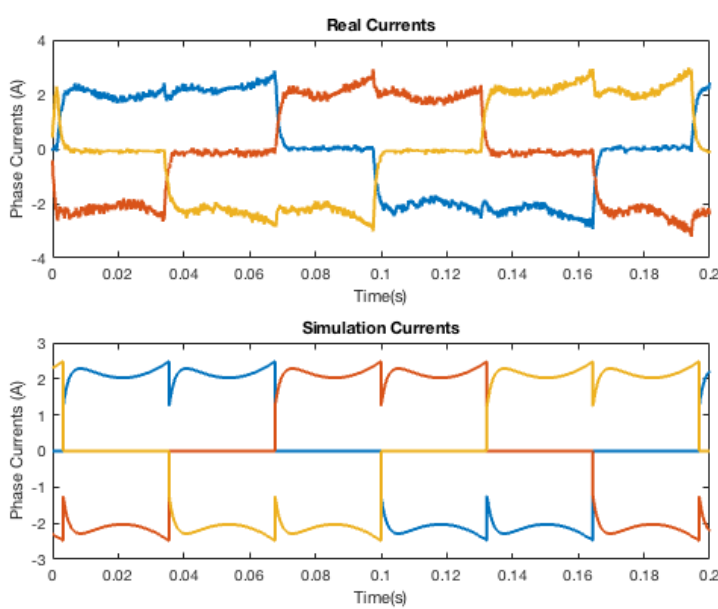


Figure 4.14: Comparison Current Phases with Duty Cycle 10% -With Load

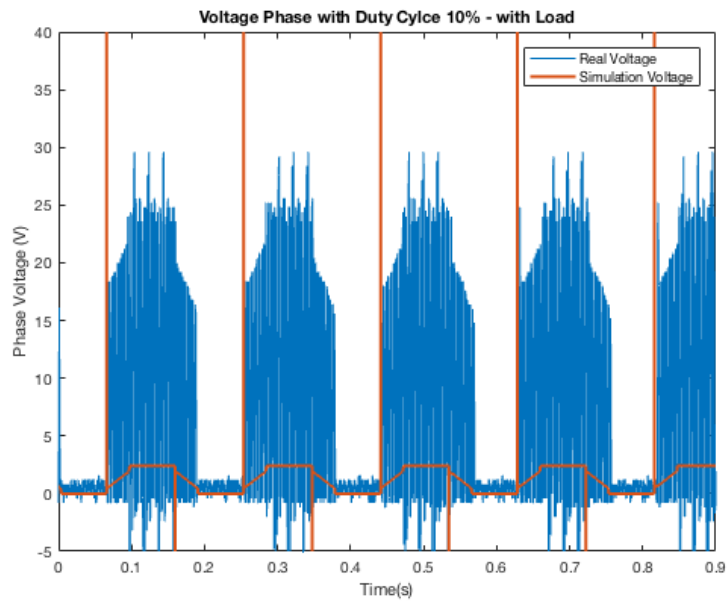


Figure 4.15: Voltage Phase with Duty Cycle 10% - With Load

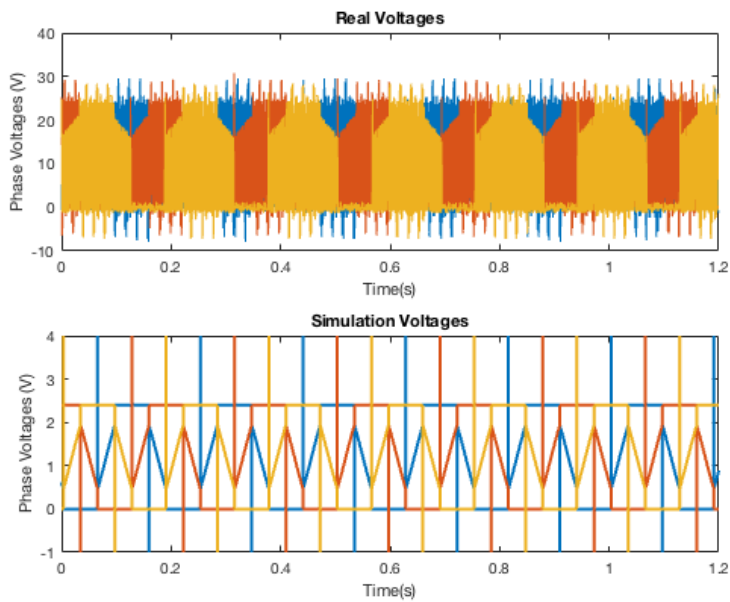


Figure 4.16: Comparison of Voltage Phases with Duty Cycle 10% - With Load

$D = 50\%$

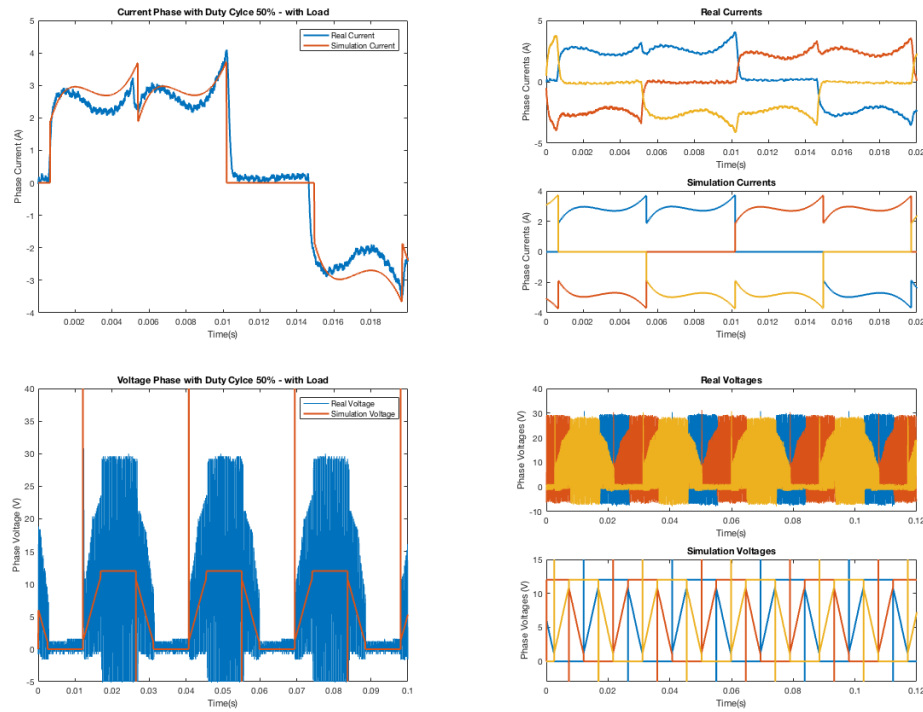


Figure 4.17: Tests with Duty Cycle 50% - With Load

2. Speed Reference at regime

In these tests we impose a reference speed and we compare currents and voltages at regime.

a. Without Load

Speed = 100 rpm

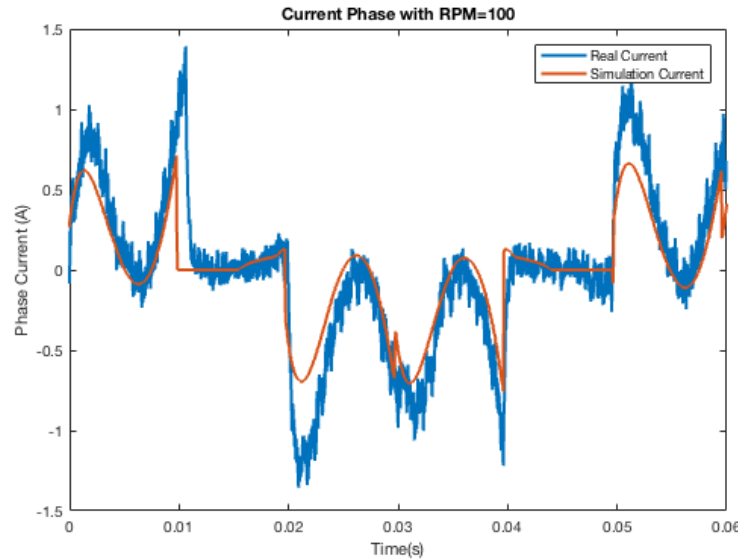


Figure 4.18: Current Phase with Speed 100rpm

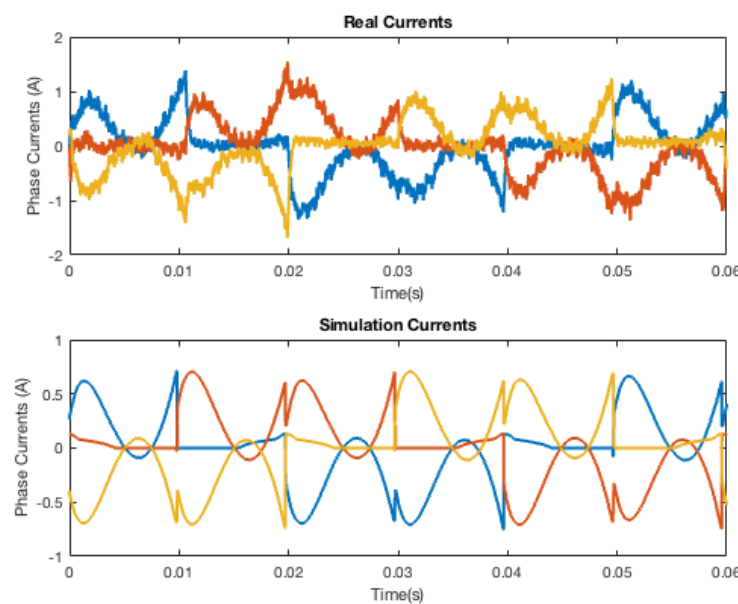


Figure 4.19: Comparison Current Phases with Speed 100 rpm

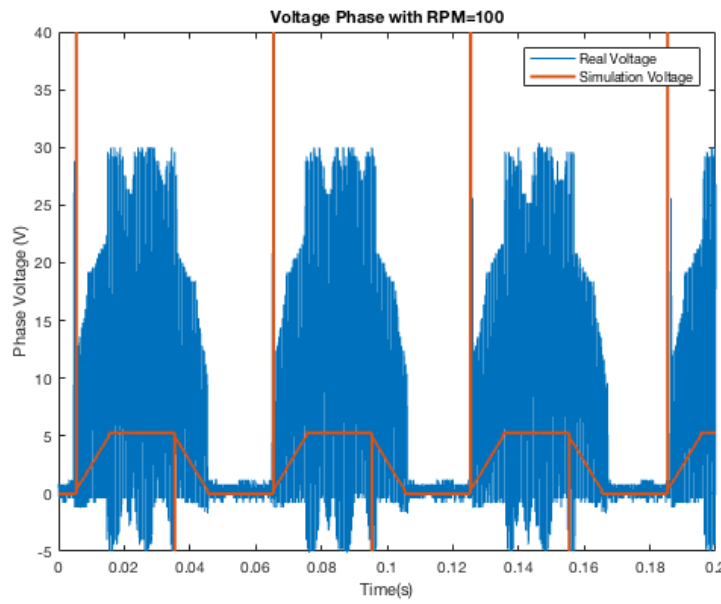


Figure 4.20: Voltage Phase with Speed 100rpm

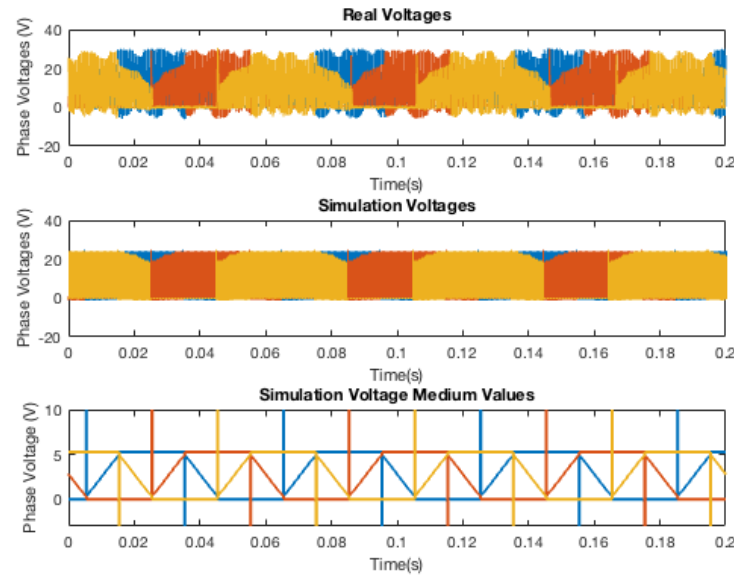


Figure 4.21: Comparison of Voltage Phases with Speed 100 rpm

4. Brushless DC Control Model

Speed = 200 rpm

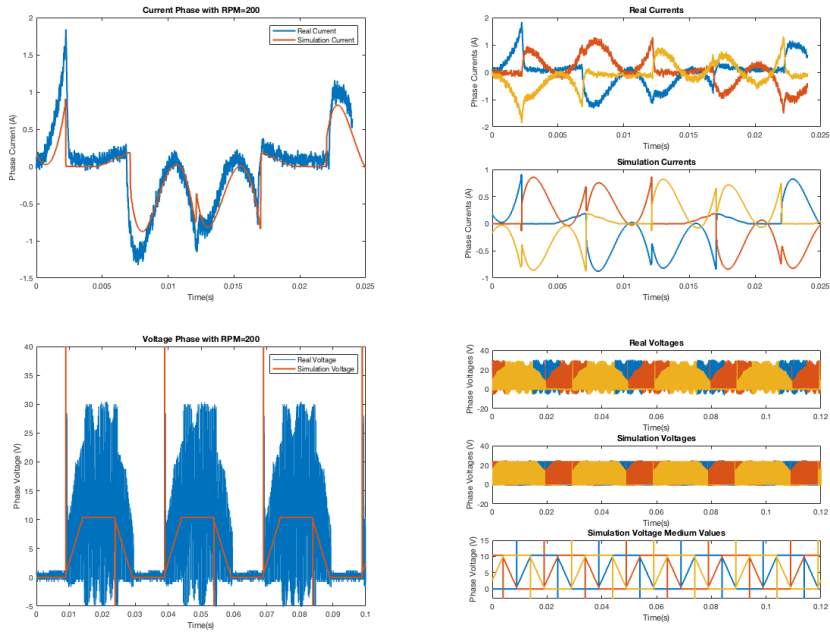


Figure 4.22: Tests with Speed 200 rpm

Speed = 400 rpm

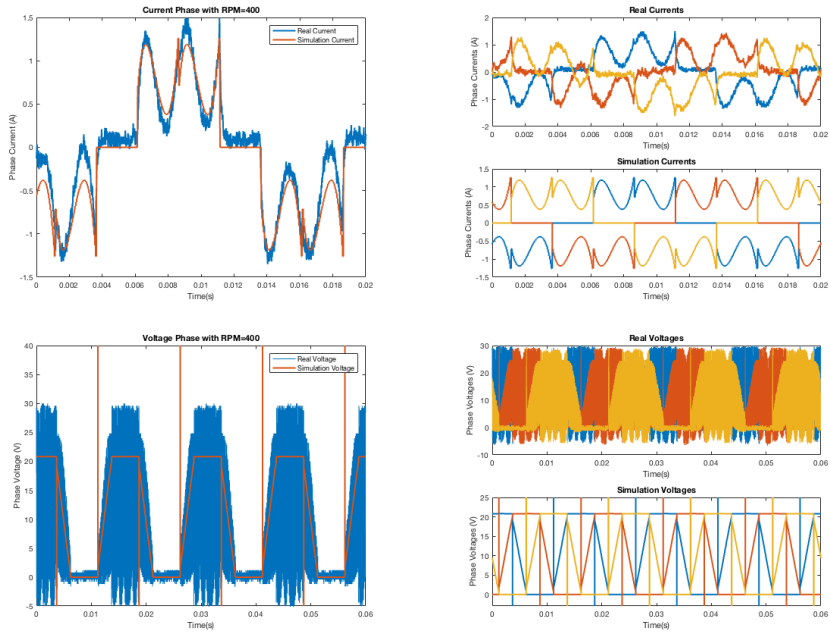


Figure 4.23: Tests with Speed 400 rpm

b. With Load

Speed = 100 rpm

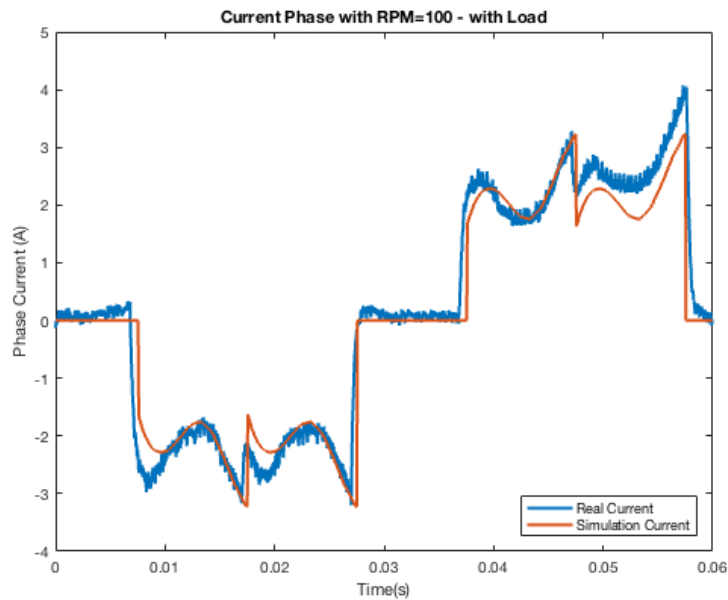


Figure 4.24: Current Phase with Speed 100rpm - With Load

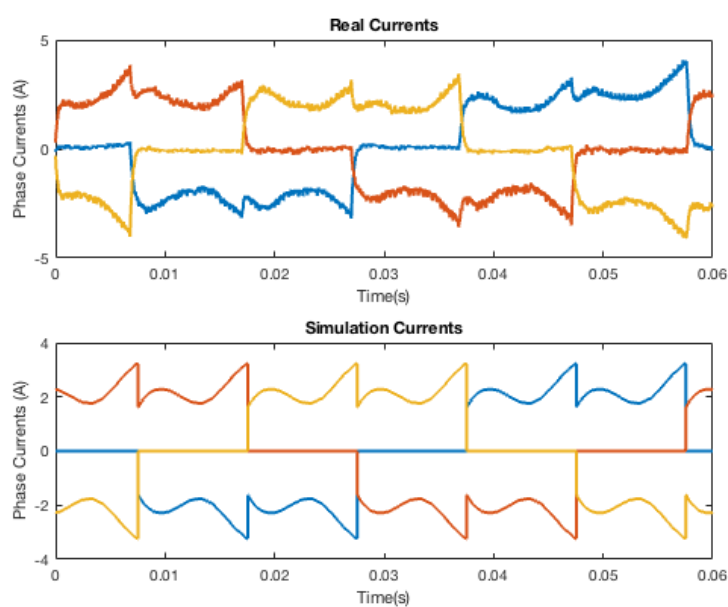


Figure 4.25: Comparison Current Phases with Speed 100 rpm - With Load

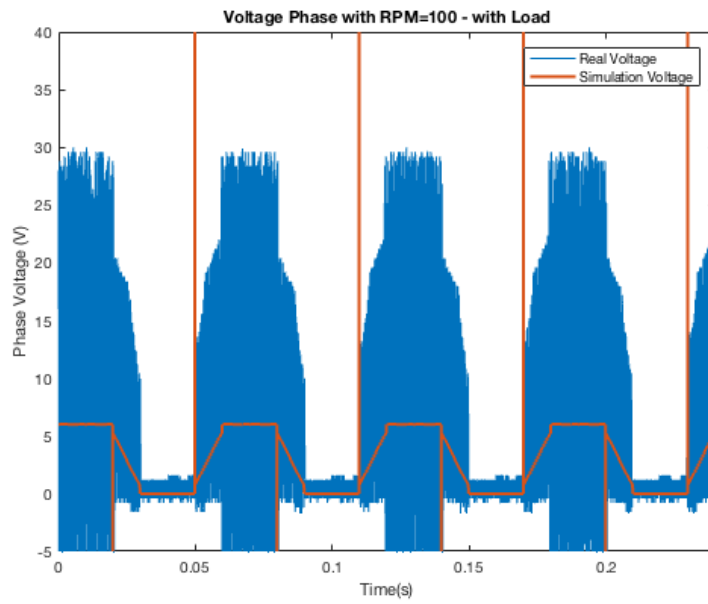


Figure 4.26: Voltage Phase with Speed 100rpm - With Load

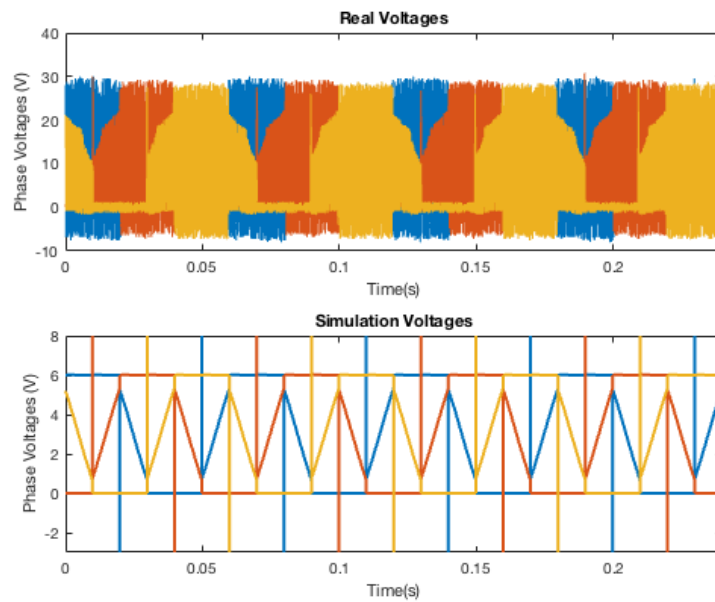


Figure 4.27: Comparison of Voltage Phases with Speed 100 rpm - With Load

Speed = 200 rpm

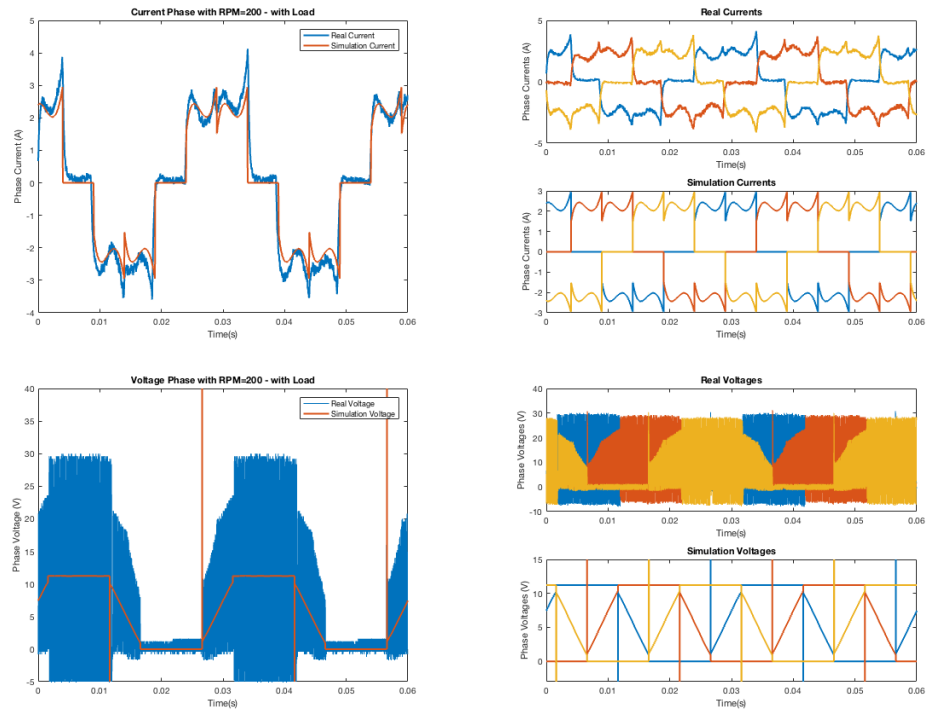


Figure 4.28: Tests with Speed 200 rpm - With Load

Speed Reference - Step Response

In this last test we look at the speed of the motor when a speed reference is imposed

Speed = 100 rpm

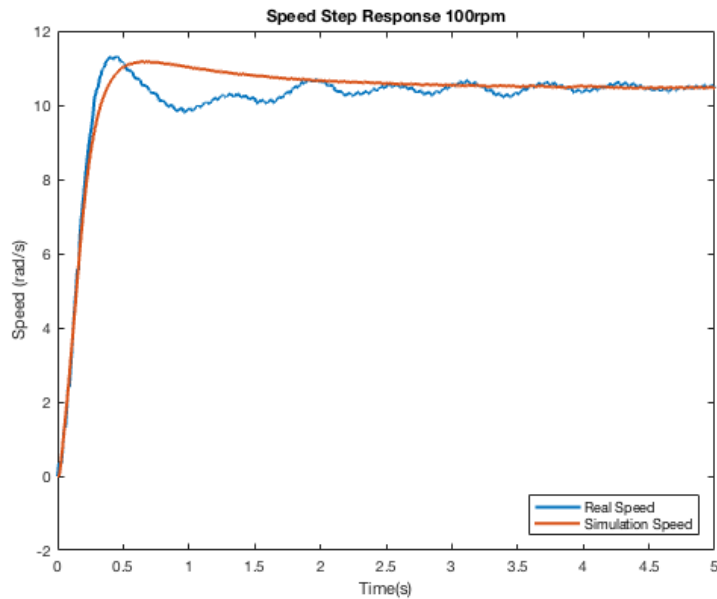


Figure 4.29: Speed Step Response 100 rpm

Speed = 200 rpm

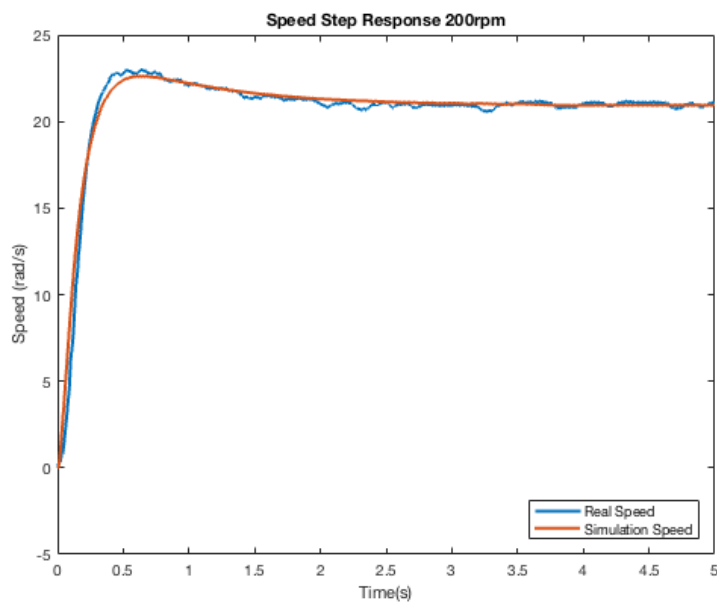


Figure 4.30: Speed Step Response 200 rpm

The simulation speed reflects the real speed in these 2 tests. In Figure 4.29 the noise of the real world is more evident with some oscillation.

4.4 Controller Parameters

The model can be now considered an approximation of the real motor, so now we have to find the best parameters to control the motor.

4.4.1 Current Loop

The electrical transfer function of the Motor, in case of BLDC Control is

$$M_{el}(s) = \frac{1}{2} \frac{1}{R + sL} \quad (4.1)$$

The control strategy is based on finding on each cycle a step to increase or decrease the duty cycle. The step is calculated on the error from reference and measured current.

$$step = K \cdot e(t) \quad (4.2)$$

So:

$$D(t) = D(t - 1) + K \cdot e(t) \quad (4.3)$$

Calculating the transfer function

$$F(z) = \frac{D(t)}{e(t)} = \frac{K}{1 - z^{-1}} = \frac{K'T}{1 - z^{-1}} \quad (4.4)$$

The equivalent transfer function in Laplace is

$$F(s) = \frac{K'}{s} \quad (4.5)$$

The open loop transfer function will be

$$L(s) = \frac{K'V_{DD}}{2s(R + sL)} \quad (4.6)$$

Closing the loop the transfer function will be

$$F(s) = \frac{K'V_{DD}}{2L} \frac{1}{s^2 + \frac{R}{L}s + \frac{KV'_{DD}}{2L}} \quad (4.7)$$

With the firmware we are using to control the motor we have only one parameter to tune the system.

We can choose ω_0 or ξ to define the value of K' .

1. $\omega_0 = \frac{R}{L}$ to have a stable system with the crossing frequency that correspond to the second pole. The damping coefficient is $\xi=0.5$ and the phase margin is $\varphi_m=45^\circ$. The corresponding K' value is

$$K' = 7.4689$$

2. $\xi = \frac{1}{\sqrt{2}}$ to have the best compromise of speed and damping. The crossing frequency is $\omega_0 = \frac{R}{\sqrt{2}L}$ and the phase margin increase to $\varphi_m=50.73^\circ$. The corresponding K' value is

$$K' = 3.7345$$

3. $\xi = 1$ to have a closed loop transfer function with 2 poles real and coincident. The crossing frequency is $\omega_0 = \frac{R}{2L}$ and the phase margin increase to $\varphi_m=63.5^\circ$. The corresponding K' value is

$$K' = 1.8672$$

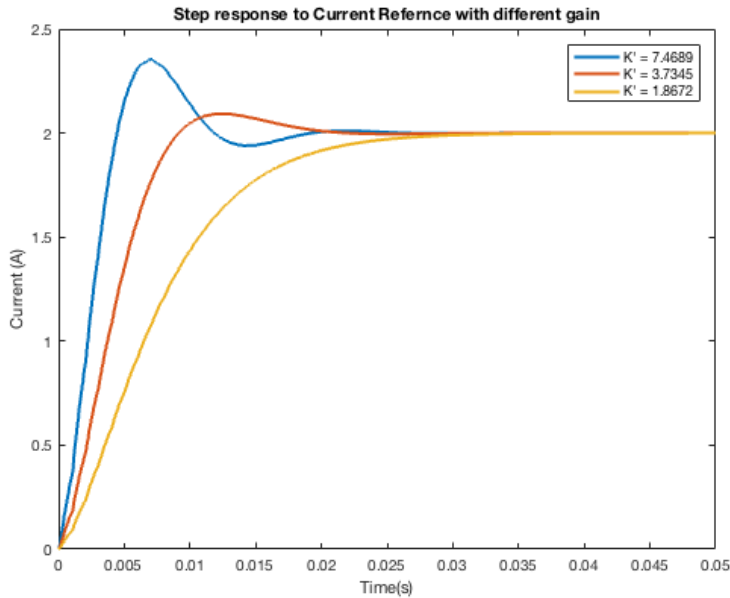


Figure 4.31: Step Response of current with different P and I values

In Figure 4.31 , as expected we can see the best choice is the second one, the fastest possible without having overshoot.

4.4.2 Speed Loop

Not depending on the control strategy, the mechanical transfer function of the motor is the same seen before in the FOC control chapter. We can still not consider the friction that help stability

$$M_{mec}(s) = \frac{1}{Js} \quad (4.8)$$

We use a PI Controller as in FOC Control and we will have the same transfer function in closed loop

$$F(s) = \frac{P}{J} \frac{s + \frac{I}{P}}{s^2 + \frac{p}{J}s + \frac{I}{J}} \quad (4.9)$$

Calculation are the same as before, but we have to consider we have a lower ω_0 depending on a lower crossing frequency in the Current Loop on Trapezoidal Control.

Using $\omega_0=34$ rad/s, 1 decade less than ω_0 of current loop, and $\xi = \frac{1}{\sqrt{2}}$ we will have

$$P = 1.4893$$

and

$$I = 25.3164$$

Instead with $\xi = 1$ we will obtain

$$P = 0.7747$$

and

$$I = 25.3164$$

In Figure 4.32 we can compare the step response of the speed in these 2 cases.

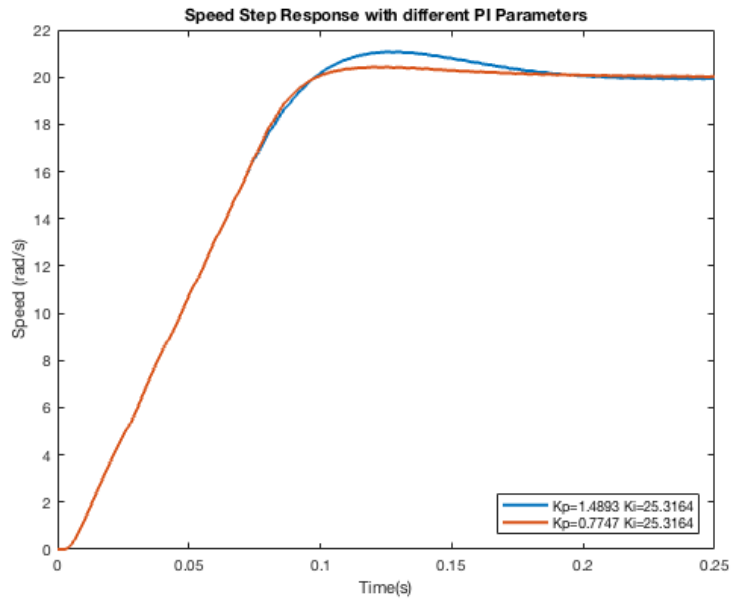


Figure 4.32: Speed Step Response with different PI Parameters

We can see more in details the overshoot of the 2 simulations in Figure 4.33 .

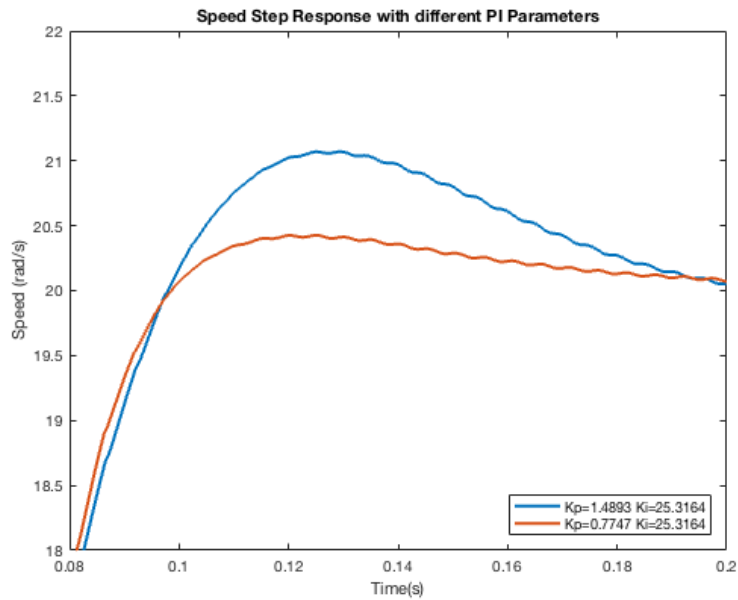


Figure 4.33: Speed Step Response with different PI Parameters - Detail

It wasn't expected an overshoot in both simulation but only in the first one, the reason can be identified in saturations not considered during calculation of parameters.

Chapter 5

Comparison between FOC and 6-Step

In this last chapter we are going to compare results obtained in the previous 2 chapters. We are going to ask ourselves which one is the better control strategy.

5.1 Speed Step Response Comparison

A test was made imposing a reference speed of 30 rad/s and looking at the step response in both cases.

In Figure 5.1 we can see the simulation made with FOC control is faster than the one with 6-Step commutation. It can be expected knowing parameters of controller. We have seen in previous chapter that with FOC controller it is possible to achieve an higher speed due to an higher crossing frequency.

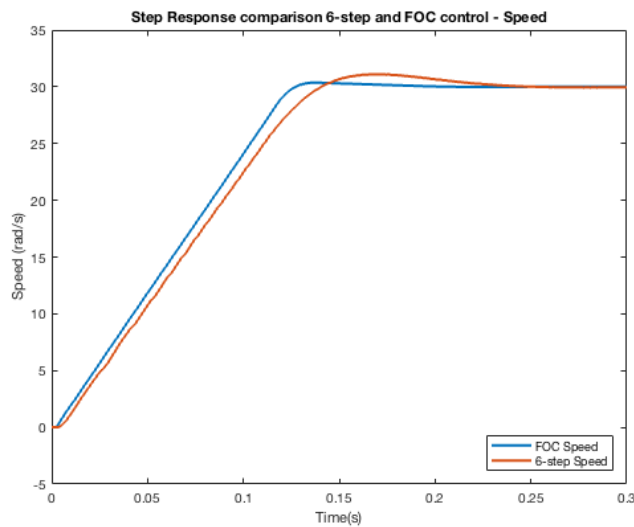


Figure 5.1: Speed Step Response with FOC and 6-Step

5. Comparison between FOC and 6-Step

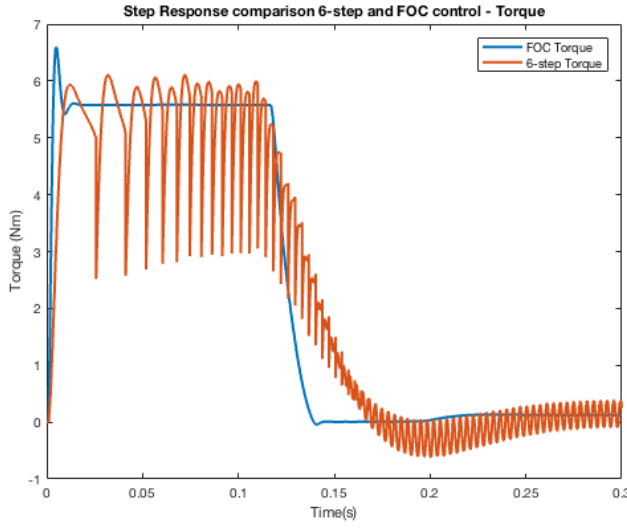


Figure 5.2: Torque during Step Response with FOC and 6-Step

In Figure 5.2 it is possible to see how the torque is enveloped on both control strategy. In both cases there is a flat zone with a constant Torque, at least as a target: with Foc this constant torque is reached, while with 6-step commutation the Torque is not constant. This is expected because the motor has Sinusoidal BEMF and if we look back at the equation 1.6 we can see the dependence of the torque from the angle between rotor and stator.

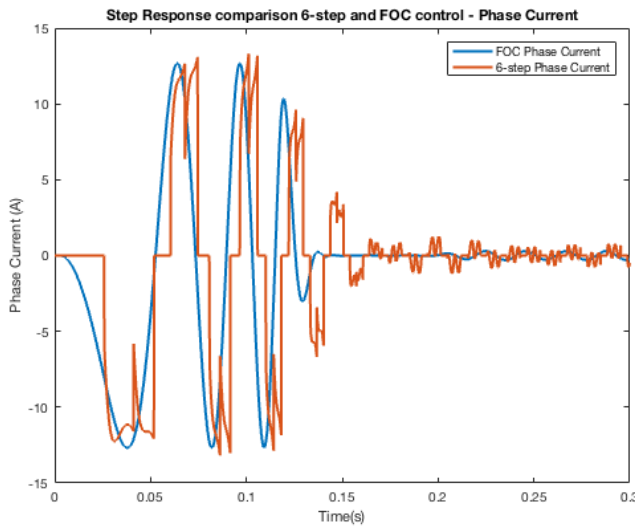


Figure 5.3: Current phase during Speed Step Response with FOC and 6-Step

Last comparison for this test is about the phase current. In Figure 5.3 we can see the difference of the 2 control strategy on the current in each phase: with Foc strategy there aren't discontinuity in current, not considering the modulation, while

using 6 step commutation it is possible to see the current going to zero alternatively. It is interesting see the shape of both control method is at the first order the same, without considering the lag increasing in 6-step due to a lower speed as we have seen in Figure 5.1 .

5.2 Comparison at Regime

Another test is made comparing torque and current at regime when the speed is constant.

In Figure 5.4 we can see better the difference in torque between 2 strategy. As before with Foc the torque is constant while with 6-step commutation the torque has a sinewave-like shape around the same value.

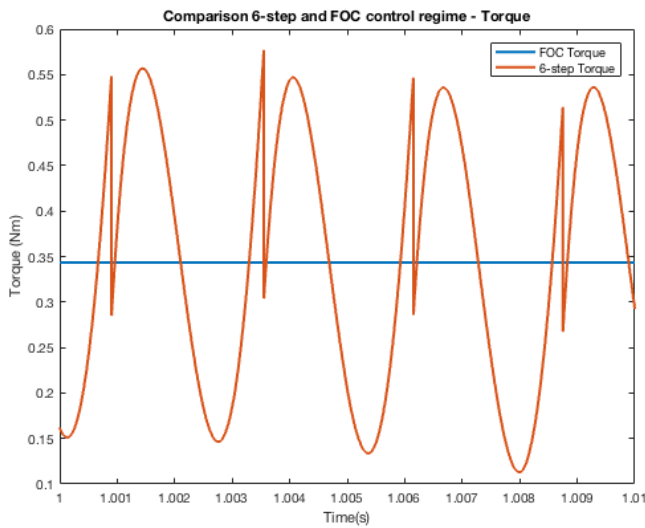


Figure 5.4: Torque at regime with FOC and 6-Step

In Figure 5.5 we can see better the phase current at regime. Ideally with Foc the current is a perfect sinewave, and this is respected in the simulation. With 6-Step commutation, if the motor has trapezoidal BEMF, the shape of phase currents should be composed like a squarewave alternate positive and negative step; actually with a sinusoidal BEMF appear a sinusoidal shape around the value we considered constant.

5.3 Choise of Control Strategy

In every figure in this chapter we can see a better behavior of the Foc strategy to control the motor: considering Figure 5.1 we can see that with parameters we have found Foc is faster then 6-Step commutation. In comparison of torque we can

5. Comparison between FOC and 6-Step

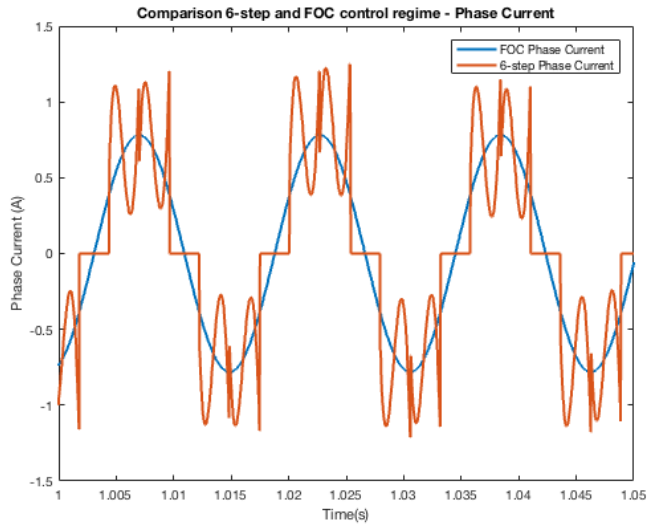


Figure 5.5: Current Phase at regime with FOC and 6-Step

see the better quality of Foc, there are no oscillation and discontinuity while with 6-Step commutation don't exist a constant torque, but just a constant medium torque value. If we need a precise control it is possible we can't afford oscillation generated in 6-Step Commutation. A little advantages is present also considering current, in Figure 5.5 we can see the peak value of phase current is bigger in 6-step commutation than in foc, having limitation of Current it becomes easier exceeded limitation of the motor if in same condition the current is bigger.

Conclusions

The purpose of this thesis was to realize a Simulink model of the in-Wheel brushless motor and its control strategy.

The first problem to solve was to understand parameters needed in simulation and to detect them from the real motor. In Chapter 2 we have found important parameters from the motor:

Parameter	Value
R_{phase}	186 mΩ
L_{phase}	386 μH
ϕ_m	29.3 mWb
J	0.0219 Kgm ²
J_{load}	0.6252 Kgm ²

Table 5.1: Parameters detected

It was also calculated the Friction as a function of angular speed both in case with and without the load.

Every parameter was then validated replicating experiments in simulation as we can see from figures in Chapter 2.

- R_{phase} and L_{phase} were validate in Figures 2.3 and 2.6
- J and Friction were validate in Figures 2.8 and 2.10
- J and Friction with load were validate in Figure 2.12

Once parameters of the motor were validated, the study focused on control strategy. First tests with both control strategies were to compare algorithms used in the firmware of real motor with calculation made in simulation. Figures from 3.9 to 3.21 for Foc and Figures from 4.7 to 4.30 for 6-Step Commutation show that both models are similar enough to real motor, as we want.

Comparisons between control strategy show that Foc should be preferable to 6-Step commutation, as shown in Chapter 5. Main problem of taking this result sure

is represented by the real world, in simulation we consider every sensor ideal: there is no noise and there isn't any delay. The real motor still have some future not considered:

1. Only two currents can be read through 2 shunt resistors. These resistors aren't on the phase but they are on the leg of the inverter. From these currents it is however possible to reconstruct phase current, but it can become problematic due to the fact we need the current flow at least one moment to ground to read its value.
2. Inverter was simplified due to long time of simulation. Too low switching frequency of the invert can make the system instable. Calculation of parameters of Controller should be done taking care of this frequency: considering a crossing frequency enough lower then switching frequency every problem should be avoided.
3. Angular position is read only with hall effect sensors. With 6-step commutation this isn't a problem, we divide the angle in 6 sectors exactly as hall effect sensors do. With Foc technic not having a perfect position can be problematic because it is needed in Park transformation.

Improvements regarding the model can be done in these 3 directions.

Bibliography

- [1] DC AN885-Brushless. Motor fundamentals. *Microchip Technology Inc*, 2003.
- [2] Nahas Basheer. Introduction to electric motors. (<https://mediatoget.blogspot.it/2012/01/introduction-to-electric-motors.html>).
- [3] Benjamin. Vesc firmware. (<https://www.vesc-project.com/node/309>).
- [4] Edison Tech Center. The electric motor. (<http://www.edisontechcenter.org/electricmotors.html>).
- [5] Marco Baur Luca Bascetta and Giambattista Gruosso. Robi: A prototype mobile manipulator for agricultural applications. *electronics*, 2017.
- [6] Gianantonio Magnani, Gianni Ferretti, and Paolo Rocco. *Tecnologie dei sistemi di controllo*. Mc-Graw-Hill libri Italia, 2000.
- [7] Nicola Schiavoni Paolo Bolzern, Riccardo Scattolini. *Fondamenti di Controlli Automatici*. McGraw-Hill, 2004.
- [8] Hamid A Toliyat and Tilak Gopalarathnam. Ac machines controlled as dc machines (brushless dc machines/electronics). *The Power Electronics Handbook*, 2002.

Bibliography
